Dynamics of therapeutic gene delivery to sensory neurons of the trigeminal ganglion

Chung H. Dang

A dissertation

submitted in partial fulfillment of the

requirements for the degree of

Doctor of Philosophy

University of Washington

2015

Reading Committee:

Keith R. Jerome, Chair

David M. Koelle

Stephen J. Polyak

Program Authorized to Offer Degree:

Pathobiology

University of Washington

Abstract

Dynamics of therapeutic gene delivery to sensory neurons of the trigeminal ganglion

Chung H. Dang

Chair of the Supervisory Committee:

Professor Keith R. Jerome

Laboratory Medicine

The development of novel therapies to treat diseases of the nervous system requires a multidisciplinary approach. Recent advances in gene therapy technologies have made it possible to accurately edit genomes *in vivo*. Editing of genomes allow scientists to replace defective cellular genes with fully functional genes to treat neurodegenerative diseases, or promote mutagenesis of essential viral genes from pathogenic viruses to inhibit infection and disease. One such pathogen, herpes simplex virus (HSV), evades antiviral immunity by establishing latency in peripheral sensory neurons where it persists as intranuclear episomes. Upon viral reactivation, HSV can cause recurrent disease and transmission to new hosts. Disruption of essential HSV genes in infected sensory neurons has the potential to prevent reactivation. The basic principle of gene therapy requires efficient delivery and expression of therapeutic genes in target cells using a safe and reliable vector system appropriate for the treatment. Viruses are natural gene delivery systems, and hence, they can be employed as therapeutic gene vectors. To

determine the dynamics of therapeutic gene delivery and expression in sensory neurons of the trigeminal ganglion, we used a viral vector derived from adeno-associated virus (AAV) in a mouse model. We found that AAV serotype 1 (AAV-1) trafficked to the trigeminal ganglion (TG) after intradermal injection in the mouse whiskerpad. Furthermore, AAV-1, 5, 7, 8, 9, which have diverse cellular tropisms, trafficked to the trigeminal ganglion from the whiskerpad with similar efficiency, although AAV-1 gave the highest levels of transgene expression. After trafficking to the TG in just 3 days, the level of AAV genomes in the TG remained constant for at least 28-days post inoculation. We determined that $5x10^{11}$ AAV vector genomes provided the highest level of AAV-mediated transgene expression in neurons, *in vivo*. Importantly, we achieved at least 50% transduction efficiency of neurons in the TG after whiskerpad injection. Moreover, the level of transgene expression was sustained for at least 28-days post inoculation. We showed that AAVs co-transduced the same neurons, which enabled delivery of multiple genes to the same target cells. In addition, we demonstrated that AAV-1 co-infect neurons that was infected with HSV-1. Understanding the parameters necessary for AAV-mediated gene transfer to neurons in the trigeminal ganglion may allow a gene therapy approach to treat HSV-1 infections, and likely other diseases that directly affect or are mediated by sensory neurons in the nervous system.

Table of Contents

List of Figures & Tables ...……...…….…....…..… iv

Acknowledgements ……...…….……...…....…vi

Chapter 1: Introduction ……..…..……..……..... 1

1.1 Adeno-associated virus (AAV) as a gene delivery vector to neural tissues

1.2 Use of AAV vectors to deliver therapeutic gene-encoded nucleases to treat HSV-1 infection in a mouse model

1.3 Herpes simplex virus type 1 life-cycle

Chapter 2: Methods …….…...…… 13

2.1 Production of AAV vectors

2.2 Quantitation of AAV vector genomes or HSV-1 viral load in the trigeminal ganglion (IHC, Quantitation & Statistical Analyses)

2.3 Viral inoculation (ocular or whiskerpad) of mice

2.4 Quantitation of transgene expression in the trigeminal ganglion

2.5 Culture of primary neurons from mouse trigeminal ganglion

2.6 Analysis of targeted mutagenesis of HSV-1 U_L19

Chapter 3: Delivery and expression of a transgene in sensory neurons of the trigeminal ganglion

Introduction ……..…….. 23

Results ……...…… 25

3.1 AAV traffics to the trigeminal ganglion by intradermal injection of the mouse whiskerpad

3.2 Effects of AAV serotypes in transduction of neurons in the trigeminal ganglion

3.3 AAV does not induce inflammation in the trigeminal ganglion

3.4 An effective dose of AAV1 is $5x10^{11}$ vector genomes

3.5 Levels of AAV genomes in the trigeminal ganglion remain constant, at least to 28-day post inoculation

3.6 AAV-mediated transgene expression increases to 28-day post inoculation

3.7 AAVs co-transduced neurons in the trigeminal ganglion

Discussion ……..…….. 41

Chapter 4: Establishing a model for targeted mutagenesis of HSV-1 infected sensory neurons

Introduction …….…… 44

Results …….…… 47

4.1 HSV-1 infection of sensory neurons of mouse trigeminal ganglion

4.2 Quantification of HSV-1 genomes in trigeminal ganglion: ocular vs whiskerpad inoculation and acute vs latent infection

4.3 Establishment of HSV-1 latency and viral reactivation

4.4 Co-infection of AAV1 and HSV-1 in sensory neurons

4.5 Treatment of HSV-1 infected mice with engineered homing endonucleases

Discussion ……..…….. 54

Chapter 5: Future Directions …….……..….….…….. 56

Bibliography……....…… 61

List of Figures & Tables

Figure 1. Schematic of genomes of wild type adeno-associated virus (AAV) and AAV vector …… 3

Figure 2. AAV-1 vectors trafficked to the trigeminal ganglion after intradermal injection of the mouse whiskerpad ……..…… 23

Figure 3. AAV serotypes 1, 5, 7, 8, and 9 trafficked to the trigeminal ganglion from the whiskerpad with similar efficiency ……...…… 25

Figure 4. AAV serotype 1 most efficiently transduced sensory neurons of the trigeminal ganglion ……... 26

Figure 5. AAV does not induce tissue damage in the trigeminal ganglion …..… 30

Figure 6. Dose response of AAV vector genomes in the trigeminal ganglion following whiskerpad injection …….…….. 32

Figure 7. Levels of AAV vector genomes remained constant in the trigeminal ganglion …….…… 33

Figure 8. Optimal AAV-mediated transgene expression in the trigeminal ganglion …….…… 35

Figure 9. AAVs co-transduced neurons in the trigeminal ganglion ……...…….. 37

Figure 10. Quantitation of HSV-1 DNA in the trigeminal ganglion ……...…… 45

Figure 11. Establishment of HSV-1 latency and reactivation of the trigeminal ganglion in mice …….…….. 46

Figure 12. AAV1 and HSV-1 co-infected sensory neurons in the trigeminal ganglion *in vivo* 48

Figure 13. *In vivo* targeted mutagenesis of HSV-1 in infected neurons in the trigeminal ganglion 50

Table 1. Gene therapy for diseases of the nervous system 5

Acknowledgements

I would like to thank Keith Jerome for the opportunity to work in his lab. I would like to acknowledge Lee Ann Campbell for allowing me to transfer into the Pathobiology Program to complete my PhD. I also want to acknowledge my thesis committee members, Michael Lagunoff, Steve Polyak, David Koelle, and Tim Rose for their support. Additionally, I would like to thank Larry Corey for his support as well.

Dedication

I dedicate this to my beautiful wife. Together we will do all that we want to do, and more.

Chapter 1

Introduction

Gene therapy of the nervous system heavily relies on viral vectors to deliver and express therapeutic encoded proteins in neural tissues. Such therapies can be utilized to correct a disease induced by a genetic mutation [1], or use to manipulate the specific neural cell for investigation. To translate to the clinical setting, such gene delivery tools must efficiently transduce their target cells, but also be replication-deficient, non-immunogenic, and have little or no cellular toxicity.

Early use of a viral vector targeted to neural cell types involved recombinant herpes simplex virus (HSV) due to its natural tropism for infecting neurons. These early HSV vectors demonstrate cellular toxicity [1, 2]. Moreover, such HSV vectors elicit higher levels of immunity from the host. These issues result mainly from viral genetic sequences that produce toxic viral proteins or contaminant gene products during production of the viral vector stocks [2]. Later generation HSV vectors are deleted of many viral genes that encode proteins directly responsible for toxic effects of some cell types, but neural toxicity still exist from such vectors. Furthermore, HSV vectors are difficult to manipulate due to their large genome, ~152 kb.

Discovery of adeno-associated virus (AAV) in 1965 proved to be very useful in the field of gene therapy decades later [3]. As a consequence of this discovery, generation of the first AAV vector occurred about twenty years later [3, 4]. Since then, it has been shown to be highly successful at transduction of different neural cell types. Subsequent iterations of AAV vectors led to the first human clinical trial in cystic fibrosis patients just ten years after the introduction of AAV vectors [5]. Today, use of AAV vectors in research and clinical trials have increased significantly.

1.1 Adeno-associated virus (AAV) as a gene delivery vector to neural tissues

The introduction of the first AAV-based vector, AAV2, appeared to induce little to no immunogenicity and was considered to be relatively non-toxic [4]. Further refinement of the AAV vector led to the current AAV-based vector that does not encode or express any wild-type viral proteins. In fact, the only viral sequences that are included in the current viral vector are the AAV inverted terminal repeats (ITRs) that flank the expression cassette (Figure 1). The ITRs are required for replication and packaging of the recombinant genome in the viral capsid to make a fully functional viral vector [1]. AAV vector stocks did not contain contaminants from helper virus during the generation of purified AAV vectors. Early tests of recombinant AAV2 vectors show no observed cellular toxicity when directly injected into the brain or spinal cord of rats, and there appeared to be low immunogenicity in small animal models [6-8]. There were no induction of cellular immune response, and only low levels of humoral immunity resulted from AAV2 [9, 10]. Importantly, introduction of transgenes into the targeted cells in the

brain show sustained and robust expression [6]. Therefore, the AAV2 vector became an attractive tool to be employ for gene therapy in research and clinical settings.

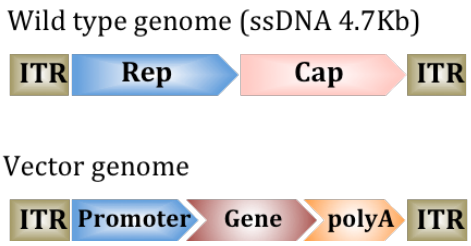

Figure 1. Schematic of genomes of wildtype adeno-associated virus (AAV) and AAV vector

Initial transduction experiments with AAV2 show that when directly injected in rodent brains, transgene expression was mostly localized at the injection site [6]. Some groups wanted more distribution of transgene expression to other parts of the brain that were difficult to access by direct injection. Because different AAV serotypes may have different cellular tropisms, various AAV serotypes may be use to target a variety of neural cell types. Therefore, more AAV serotypes were introduce to improve gene delivery to different neural cell populations in the brain. For example, when comparing AAV5 versus AAV2 after direct injection in the brain, AAV5 show more variable and disperse transgene expression patterns than AAV2 [11, 12]. AAV2 transgene expression was more concentrated at or around the site of injection in the brain. In contrast, when AAV2 or AAV5 was injected in the retina to transduce photoreceptor cells, it was reported that AAV2 had a more dispersed transgene expression profile than AAV5

[13,14]. These reports suggests that the transgene expression profile of neural tissues in the brain or retina is affected by, both, AAV vector serotypes and injection routes.

The transduction efficiency of AAV vectors could likely rely on the expression levels of serotype-specific entry receptors on the cell surface of the targeted neural cell. Due to the asymmetric nature of the structure of neurons, AAV entry receptors may not be evenly distributed throughout entire cell surfaces of various neural cell types. For example, nerve terminals could express different levels of surface entry receptors than cell bodies of neurons. Therefore, efficient transduction of specific neural cells could require that AAV entry receptors be expressed at the cell surface region where they are accessible at the injection site.

Administration of therapeutic AAV vectors to transduce specific neural cells could likely be dictated by the specific disease pathology of the nervous system. For example, in cases where the disease is associated with loss of neurons such as Alzheimer's disease or Parkinson's disease (Table 1), the encoded gene delivered may produce a survival factor [16]. Hence, the injection site must be close to the neuronal cell bodies where the survival factor can quickly prevent cell death. In other situations, where the desire effect is to induce axonal growth or projections towards the site of traumatic injury, one might administer the AAV vectors at the site of injury and away from the neuronal cell bodies.

It is important to consider the desire therapeutic effect to determine where to inoculate the AAV vectors and how to express the transgene. For example, during traumatic injury in the peripheral nervous system, short bursts or transient levels of

therapeutic transgene expression may be sufficient. In contrast, in Parkinson's disease, one might want a constant level of transgene expression in dopaminergic neurons located in the brain to inhibit neuronal cell death [16].

AAV vector-mediated gene therapies that involve the nervous system require precise injection of viral vectors to target neurons due to most neurons' asymmetric architecture. Moreover, diseases that affect different parts of the nervous system, i.e., central vs peripheral, would likely direct one to where to inject AAV vectors and which AAV serotype to use for efficient transduction of target neurons. Expression of viral vector-mediated knockdown of cellular genes of interests would enable a wide range of investigations on gene function, such as axonal growth or synapse formation of neurons, mainly in the brain. In the peripheral nervous system, one could use viral vector technology to study how nerve regeneration can occur by manipulation of cellular gene function.

Table 1. Gene therapy for diseases of the nervous system

Gene therapy for diseases of the nervous system	
Therapy	Disease or Injury
Increase axonal growth and synaptic plasticity	Alzheimer's Nerve damage Parkinson's
Prevent neuronal death	Alzheimer's Parkinson's Ischemia / stroke
Stimulate remyelinization	Multiple sclerosis

Currently, AAV vector-mediated gene delivery has been successfully applied to a number of rodent models of human disease. In mice, AAV vector-mediated expression of beta-glucuronidase subdued formation of brain lesions which models a human disorder of lysosomal storage [15]. In the rat model of Parkinson-like disease, AAV vectors have been used to deliver glial cell line-derived neurotrophic factor (GDNF) to counteract neuronal cell degeneration [16]. Furthermore, AAV vectors have been used to encode genes that express anti-apoptotic proteins such as bcl-2 in mice models of amyotrophic lateral sclerosis (ALS) [17]. Instead of inhibiting neuronal death, AAV vectors have also been employed to induce cell death by encoding a suicide gene such as thymidine kinase to induce brain tumors in mice and rat models [18]. Based on the successful applications of AAV as a gene delivery vector to treat diseases of the nervous system, we aimed to utilize AAV vectors to deliver gene-encoded therapeutic nucleases to treat herpes simplex virus type 1 infected neurons in a mouse model.

1.2 Use of AAV vectors to deliver therapeutic gene-encoded nucleases to treat HSV-1 infection in a mouse model

We are interested in using AAV-based vectors to deliver gene-encoded nucleases designed to promote mutations of essential HSV-1 genes, thus disabling HSV-1. In most HSV-1-infected individuals on antiviral therapy, viral replication is suppressed. However, HSV-1 persists in a latent form in peripheral sensory neurons of the trigeminal

ganglia and can reactivate to cause recurrent disease and infect others. In order to cure HSV-1 infected individuals, one has to prevent viral reactivation.

We hypothesized that targeted mutagenesis of essential HSV-1 genes in latently infected sensory neurons could prevent viral reactivation. The laboratory has previously demonstrated this for HSV using an in vitro model [90], and for HIV and HBV using similar culture models [91]. We therefore proposed to investigate targeted mutagenesis of HSV-1 in infected sensory neurons, *in vivo*. In this context, we established a mouse model of HSV-1 infection to determine parameters required for directed mutagenesis of target sites in HSV-1 genomes in infected neurons. Critical to our goal is the ability to deliver therapeutic gene-encoded nucleases to HSV-1 infected neurons in the trigeminal ganglion.

As proof of concept, we used targeted nucleases to impair essential viral genes in HSV-1 infected neurons, *in vivo*. Homing endonucleases (HEs) are a class of such nucleases that can be utilize to trigger directed mutagenesis of a specific target site. Discovered in the 1970s, homing is a gene conversion process that involves the insertion of a copied mobile sequence into its cognate allele that lack this sequence [19]. Therefore, a site-specific double strand break (DSB) in the target allele is required by a "homing endonuclease" that is encoded within the mobile sequence. HEs recognize very long DNA sequences (14-44 bp), which give them exquisite specificity [19]. To deal with DSB, cells have three major DNA DSB repair mechanisms: non-homologous end joining (NHEJ), microhomology-mediated end joining (MMEJ), and homologous recombination (HR). In absence of a homologous repair template, NHEJ is favored. Moreover, NHEJ is the predominant DNA DSB repair pathway in higher eukaryotes.

Imprecise repair during NHEJ can result in mutations at the target site caused mainly by insertions or deletions. Under this premise, we employ engineered HEs to trigger target site mutagenesis within the HSV-1 genome. Then, we analyze the target sites to confirm the effectiveness of our approach.

Although, there are currently four classes of nucleases that may potentially have therapeutic effects we tested engineered homing nucleases (HEs) in this study. We have chosen to initially test HEs *in vivo* because of their small size thus allowing us to easily package the open reading frame in the AAV vector genome. Moreover, the high specificity of HEs to our desired HSV-1 target site would likely result in lack of cellular toxicity. Other nucleases such as Zinc finger nucleases (ZFNs), TAL effector nucleases (TALENs), or the CRISPR/Cas system may be utilized to similar ends but effective vectorization of these enzymes to specific neural tissues will require further investigation.

1.3 Herpes simplex virus type 1 life-cycle

Most humans are infected with herpes simplex virus type 1 (HSV-1) during childhood or adolescence, and remain latently infected throughout life. Serology and detection of HSV-1 DNA in their trigeminal ganglia (TG) demonstrate that by age 60, close to 80% of the world's population is latently infected with HSV-1 [22-25]. Primary infection occurs when HSV-1 enters epithelial cells of the mucosa of the mouth, where a lytic phase of primary infection develops. Following replication at the mucosa, viral particles encounter nerve termini that innervate the site of primary infection. Viral particles are then translocated via retrograde axonal transport to the neuronal cell body

where the virus establishes latency [21]. HSV-1 evades antiviral immunity by establishing latency in neurons, a phenomenon in which viral genomes persist as intranuclear episomes for life.

Typically, herpetic lesions (cold sores) result from a productive infection at the mucosal surface. When HSV-1 infection occurs in the eye it may result in keratitis, irreversible corneal scarification following several rounds of reactivation that may lead to blindness [21]. Recurrent HSV-1 is the leading cause of infectious corneal blindness in the U.S. [20]. In some cases encephalitis can ensue when HSV-1 infects the central nervous system (CNS). Herpes simplex encephalitis is often fatal [21]. Thus, recurrent HSV-1 infections can progress to serious disease, morbidity, and even mortality in the infected person's lifetime.

Recurrent disease from HSV-1 reactivation can occur intermittently and at random. Following reactivation, the virus tends to re-enter the stratified squamous epithelium layer, where many sensory neurons innervate, and emerge on the skin surface to form lesions [26]. Factors that affect the frequency of recurrence and severity of symptoms include host immunity and strain of virus. For example, immunocompromised individuals may have higher recurrence rate of HSV-1 reactivation [26]. It was suggested in the Pica *et al.* study that individuals who report the highest frequency of recurrent HSV-1 infections had much lower IFN gamma production compared to those who reported less recurrences [27].

HSV-1 establishes lifelong neuronal latency, which can be easily detected in the trigeminal ganglia (TG). When HSV-1 latency is established in the infected neuron of

the TG, HSV-1 dsDNA genomes are maintained during latency from 1 to ~50 copies of non-integrating circular episomes latently in infected neurons [37, 40]. The genome of HSV-1 is composed of 152 kb, and is divided into two unique regions (unique long and short or U_L and U_S). Each unique region is bracketed by inverted repeats. The latent viral genome is transcriptionally repressed, except for the latency associated transcripts (LATs) [28-31]. LATs are a set of linear RNAs transcribed from within internal repeat regions located between the unique long and short portion of the viral genome. During neuronal latency, viral transcription leads to a 8.3 kb primary transcript that is further processed to produce stable 2.0 kb and 1.5 kb introns [32]. Such transcripts, along with the circularized HSV-1 genomes, remain in the nucleus of the latently infected neuron for life.

Although LAT is not required for establishment of latency, many studies have shown that it plays a significant role in the establishment and maintenance of latency [33, 34]. Some studies have demonstrated that mutant viruses deleted for LAT show a reduction in the efficiency of virus reactivation *in vivo*, suggesting that LAT may be directly involved in viral reactivation [35, 36]. However, other studies that examine the murine HSV-1 latently neuron showed that LAT-negative viruses establishes latency in ~1/3 as many neurons compared to wild-type HSV-1 and this correlates with the amount of virus recovered after reactivation [37-41]. The debate in the mechanism of how LAT regulates latency and reactivation may be due to variatoins in latency models and experimental conditions in different studies. Related to this thesis, what is important to note is that regardless of the functional roles of LAT throughout latency and reactivation, the ability of the latent viral genome to enter lytic replication and cause recurrent disease

in the periphery can occur independent of LAT.

Evidence of HSV latency in nervous tissue of small animal models has been established for more than three decades. The murine model for HSV-1 infection and latency is an attractive model because it recapitulates most aspects of HSV-1 life-cycle. It can establish infection at peripheral sites similar to humans, and importantly it establishes latency in sensory neurons of the mouse trigeminal ganglia (TG) for life [35]. Thus, we exploited the mouse model of HSV-1 neuronal latency to explore our targeted mutagenesis approach of latent viral genomes.

Critical to our ability to test the hypothesis of targeted viral gene disruption *in vivo* is to determine the dynamics of therapeutic gene delivery to HSV-1 infected neurons in the trigeminal ganglion. Utilizing the AAV-based vector, the objective of my doctoral research was to quantitatively detail important parameters to enable effective delivery and robust expression of gene encoded therapeutic nucleases to neurons in the trigeminal ganglion. The rationale for this approach was two fold: 1) AAV-based vectors are easily generated, well tolerated, and able to efficiently transduce neurons; 2) Quantitative understanding of gene delivery to sensory neurons in the trigeminal ganglion is necessary to test targeted mutagenesis of latent HSV-1 infection, and potential treatments for other nervous system related diseases.

My study of gene delivery dynamics to sensory neurons of the trigeminal ganglion has revealed that AAV-base vectors can be employed to effectively transduce neurons in the trigeminal ganglion. Moreover, I qualitatively and quantitatively described optimal parameters for: route of administration, AAV serotype, viral vector

dose, kinetic of transgene expression, co-transduction efficiency of AAVs, and co-infection of AAV1 and HSV-1. Importantly, this established mouse model allowed us to demonstrate, for the first time, viral gene disruption of HSV-1 infected neurons *in vivo*.

Chapter 2

Methods

2.1 *Production of AAV vectors*

AAV vector plasmids, pscAAV-CMV-mCherry or pscAAV-CMV-GFP (provided from Daniel Stone at FHCRC, Seattle, WA), were generated by restriction digest with BgIII and cloned to pscAAV-CMV-pA. Plasmid pscAAV-CMV-HSV1m5 (provided by Martine Aubert at FHCRC, Seattle, WA) were generated by PCR amplification of HSV1m5 using primers KpnI-HA-nls GAGATCGGTACCGCCGCCACCATGGGATATCCATACGATGT and XhoI-HSV1m5 GAGATCCTCGAGTCAAGGACTTTTTCTTCTCAGAGA. Each PCR amplicon were cloned into pscAAV-CMV-pA as an XhoI-NotI fragment.

AAV viruses were generated by transient transfection of HEK 293T cells (American Type Culture Collection) using polyethylenimine (PEI) according to method of Choi et al 2007. HEK 293T cells were cultured in DMEM with 10% FBS. To maximize titers of AAV viruses, two hours before transfection, replaced old growth media to fresh growth media. When HEK 293T cells are ~60% confluent, used PEI (1mg/ml) to transfect cells (1.6 x10^7 cells per 15cm tissue culture dish). Use a ~1:1:1 molar ratio of AAV helper plasmid to Ad helper plasmid to rAAV plasmid containing the reporter or nuclease transgene per 15cm tissue culture dish for AAV serotypes 1, 5, 7, 8,

or 9. Add the DNA mixture to 500ul of pre-warmed Optimem II medium per dish. Once the plasmids are thoroughly mixed, add the PEI and vortex for 10 seconds to allow efficient transfection of all plasmids proportionally. Incubate for 5-10 minutes at room temperature and add the mixture (DNA+PEI), drop-wise to each dish. At 72 hours post-transfection, harvest crude AAV lysates by collecting and resuspending the cells in AAV lysis buffer (50 mM Tris, 150 mM NaCl, pH 8.5) before freeze-thawing four times. Filtered AAV stocks through a 0.45μm filter and stored at -80 ^{o}C.

To purify AAV vectors for *in vivo* inoculations, allow the virus suspension to thaw to 37 ^{o}C. Add benzonase (10-50 U/ml)and incubate the virus suspension at 37 ^{o}C for one hour to degrade extra-cellular DNA. Mix every 15 minutes to break down DNA to reduce the viscosity of the solution, which will aid separation of constituents in the subsequent gradient. Centrifuged the virus suspension at 3,000xg for 15 min at 4 ^{o}C. Build an iodixanol gradient in a Beckman quick-seal centrifuge tube by preparing solutions for four different layers of the gradient, i.e., 15%, 25%, 40%, and 54%. Add phenol red to the 25% and 54% layers to aid visualization of the layers within the tube. Start by adding the 15% solution to the bottom of the Beckman tube using a 10 mL syringe. Add subsequent layers below the previous layer, 25% → 40% → 54%. Add the virus containing supernatant to the gradient slowly. Seal the tip of the tube. Centrifuge the tube at 49,000 rpm in a Beckman Type 70Ti rotor for 1 hours 20 minutes at 4^{o}C. Insert an 18-gauge needle near the top of the tube to allow airflow vent. Prepare a 5 mL syringe with an 18-gauge needle for extraction of the virus-containing layer. Accurately insert the needle approximately 1-2 mm below the interface between the 40% and 54% gradient buffer layers with the bevel of the needle facing up. The AAV vectors are

visible as a subtle presence of color at the interface. Slowly extract 3 mL of solution, first with the beveled needle opening facing upwards during the first half of extraction, and facing downward for the rest of the solution. This layer represents the pure AAV virus stock.

2.2 *Quantitation of AAV vector genomes and HSV-1 viral load in the trigeminal ganglion*

Total DNA from the mouse trigeminal ganglia was extracted using the DNeasy Tissue & Blood kit (Qiagen) after surgical removal from the mouse. Quantitation of AAV vector genomes in the trigeminal ganglion by real-time PCR uses primers AAV ITR-Forward, 5'-GGAACCCCTAGTGATGGAGTT-3' and AAV ITR-Reverse, 5'-CGGCCTCAGTGAGCGA-3' and probe set AAV ITR-Probe 5'-FAM-CACTCCCTCTCTGCGCGCTCG-BHQ1-3' that will amplify a sequence within the 5' ITR of AAV2. This AAV ITR-Forward primer is designed so that it will not bind to the deleted ITR sequence found in AAV vectors or to the right hand ITR. Therefore, all AAV vectors can be titer in the same assay with only a single ITR amplified per virus and the same standard curve can be used for all AAV comparisons.

To generate PCR standard, linearized plasmid pAAV-CMV-GFP (7017bp) with DraIII restriction enzyme. Digest 5µg of pAAV-CMV-GFP in a 50µl volume for 3-4 hours. Purify the linearized DNA, and confirm that the plasmid is completely linearized on a 1% agarose gel. Quantify sample using the nanodrop and then determine the plasmid copy number per µl. In a 50µl volume place 5µl AAV sample, 5µl NEB buffer 3, 1µl DNase (40U/µl) before incubating at 37^{o}C for 30 minutes. Heat-inactivate the

DNase at 75°C for 10 minutes. Add 50µl of 2X proteinase K buffer (10mM Tris-HCl pH8, 20mM EDTA pH8, 20mM NaCl) and 10µl proteinase K (10mg/ml) and incubate at 37°C for 1 hour. Heat-inactivate the proteinase K at 95°C for 20 minutes. Dilute the sample to 1:20 and 1:100 in dH_20 before using it in qPCR reaction.

To determine AAV vector titer, dilute plasmid standard curve (10^8, 10^7, 10^6, 10^5, 10^4, 10^3 and 10^2 copies). Using TaqMan® Universal Master Mix II, with UNG, include AAV ITR-Forward (100nM), AAV ITR-Reverse (340nM), AAV ITR-Probe (100nM) and run PCR cycle 50°C for 2 minutes, 95°C for 15 minutes, then 40 cycles of 95°C for 1 minute and 60°C for 1 minute. Use SDS software to obtain a value for the number of AAV copies per sample based upon dsDNA linear AAV plasmid sample. Each PCR reaction contains 20% of total volume of DNA extracted from the mouse trigeminal ganglion.

To assess HSV-1 DNA in trigeminal ganglion, a duplex digital PCR was performed to measure the levels of cellular HSV DNA on the QX100 droplet digital PCR system (Bio-Rad Laboratories, Hercules, CA) at the University of Washington, Department of Laboratory Medicine, Molecular Virology Laboratory. DNA samples were extracted from trigeminal ganglia as described above. Copies of HSV-1 DNA were quantified using the following gB primers/probe set: HSV-qPCR-F CCGTCAGCACCTTCATCGA; HSV-qPCR-R CGCTGGACCTCCGTGTAGTC and probe HSVgbProbe 6FAM-CCACGAGATCAAGGACAGCGGCC-BHQ1. Cell numbers were determined using GAPDH primers specific to murine DNA. The ddPCR reaction mixture consisted of 12.5 ul of a 2X ddPCR Mastermix (Bio-Rad), 1.25 ul of each 20X primer-probe mix, and 10 ul of template DNA in a final volume of 25 ul. 20 ul

of each reaction mixture was loaded onto a disposable plastic cartridge (Bio- Rad) with 70 ul of droplet generation oil (Bio-Rad) and placed in the droplet generator (Bio-Rad). The droplets generated from each sample were transferred to a 96-well PCR plate and PCR amplification was performed on a 2720 Thermal Cycler (Applied Biosystems, Carlsbad, CA) with the following conditions: 95°C for 10 minutes, 40 cycles of 94°C for 30 seconds and 60°C for 1 minute, followed by 98°C for 10 minutes and ending at 4°C. After amplification, the plate was loaded onto the droplet reader (Bio-Rad) and the droplets from each well of the plate were automatically read at a rate of 32 wells/hour. Data were analyzed with QuantaSoft analysis software and quantitation of target molecules presented as copies/ul of PCR reaction. For quantification of both cellular and supernatant HSV-1 levels values were standardized to cellular GAPDH levels. Alternatively, calculations for HSV-1 DNA in one trigeminal ganglion was obtained by normalizing to 20% of total DNA tested.

2.3 *Viral inoculation (ocular or whiskerpad) of mice*

Female Swiss Webster mice (Charles River), 4-8 weeks of age, were used throughout these studies. For ocular inoculation via scarification of the cornea, 5 microliters of inoculum containing $2x10^5$ - $5x10^6$ PFU of HSV-1 KOS or F was pipetted to the cornea following scarification with an 18-gauge needle. HSV-1 production and storage according to method of Pomeranz and Blaho 2000. Tittering of HSV-1 uses method according to Roizman and Knipe 2001. HSV-1 concentration is expressed as plaque forming units (PFU). For intradermal injection of the mouse whiskerpad, 50 microliters of inoculum was injected using an insulin syringe (30-gauge needle).

2.4 *Quantitation of transgene expression in the trigeminal ganglion*

Immunohistochemistry

Using a semi-automated approach to analyze by immunohistochemistry (IHC) and cell image analysis software of histology sections of trigeminal ganglia. For IHC, trigeminal ganglion (TG) was fixed in with 10% neutral buffered formalin, paraffin embedded then sectioned at 4 um thickness. Staining of mCherry TG slides required antigen retrieval for 12 hours at pH9 in a 65 C water bath. Anti-mCherry antibody (dilution 1:1000) was made at the FHCRC (provided by Benjamin Hoffstrom). To detect mCherry, a polymer (PowerVision Rabbit HRP) was utilized along with the chromagen DAB+ Dako for 4 minutes 2 times. Counterstain with Biocare Hx and Tacha's at 25% for 2 minutes. Isotype controls of mouse Ig (1.3 ug/mL) were used as negative control. For anti-NeuN (clone A60, Millipore mab377) staining (antibody dilution 1:800), TG required antigen retrieval at for 12 hours at pH9 in a 65 C water bath. To detect NeuN, PowerVision Rabbit HRP polymer was used along with a M-E Kit (Vector Laboratories BMK #2202). Isotype controls of mouse Ig (1.3 ug/mL) were used as negative control.

Image quantitation

CellProfiler cell imaging software extracts a large number of different measurements of histology tissue stained with anti-NeuN, anti-mCherry. Images were scanned at 40x (Aspera) and captured at fixed exposure and position using ImageScope software. Individual measurements can be exported to a spreadsheet for further data processing using Microsoft Excel. To classify based on morphology, reporter intensity,

size, and other cellular characteristic, we use Classifier tool located in CellProfiler Analyst (CPA) to train a machine-learning classifier. Furthermore, based on a Boolean method of categorizing, CellProfiler automatically determines the best combination of measurements for discriminating between different phenotypes. Based on observed exclusion criteria, modifications within CellProfiler pipeline was used to classify the counted objects by mean intensity. Images determined artifacts were excluded from analysis. Stacks of images were merged with the original image in ImageJ to produce the last photo in the series to form the spatial patterns of the mean intensities.

In order to set the parameters in CellProfiler Analyst (CPA), a database of attributes important to the characteristics of the trigeminal ganglion were generated. To generate the total percentage of mCherry positive or GFP positive neurons in the image of the trigeminal ganglion, unique numbers were assigned to every countable neuron in the histology tissue. To confirm CellProfiler's accurateness at assigning valued criteria to the digital map, a set of such sections were used to verify that the CellProfiler achieved a 95% confidence level at. Export CellProfiler to an SQLite database to enable the measurements in the database to be further explored using CPA. When creating a CellProfiler listing, select the option to create a "properties file" output in the 'ExportToDatabase' module. The properties file is a simple text file that describes where raw data and extracted measurements are located when launching CPA. Edit the CellProfiler properties output file in a regular text editor.

CellProfiler Analyst was originally designed for fluorescent images of cells, so a few modifications are needed to optimize viewing of brightfield images of neurons in the trigeminal ganglion, which are also often larger than most other cell types. Moreover, the

irregular shapes and positive stained axons have to be considered. The following additions/changes to the properties file are needed prior to launching CPA (each on separate lines and without the brackets):
[image_channel_colors = red,green,blue,red,green,blue] [channels_per_image = 3,3] [image_channel_blend_modes = subtract, subtract, subtract, add, add, add] [image_tile_size = 250]. The Classifier tool of CPA needs to be trained to recognize neuron phenotypes such that CPA can determine the likelihood that a given section shows neurons belonging to specified characteristics. Training of the software to further confirm what is truly a positive neuron for the stain marker, versus an artifact of IHC is key to allow accurate CPA output. Limit the output data to detail: Image Number, Object Number, Intensity of Stain, Location of Neuron, Total Number of Positive, and Total Number of Negative. Test the classification accuracy by fetching cells of a particular class of defined labels. Such CPA enrichment scores can be visualized as a table, heat map, histogram, scatter plot, etc. Select some images that have suitable ranges of intensities so that manual selection of the boundaries of the categories can be created. Use the ranges in both the python script that to categorize all the files and create a set of images to determine an output of percentage of neurons positive for desired reporter.

Statistical analysis

Results are presented as p-values and correlation coefficient r using software MatLab. To test for differences in transduction efficiency, non-parametric one-way

ANOVA test was utilized. To compare efficacies across individual serotypes the ANOVA was followed by a multiple comparison post-test.

2.5 *Culture of primary neurons from mouse trigeminal ganglion*

Six-week-old female Swiss Webster mice (Charles River)) were euthanized (by CO_2) and the trigeminal ganglia (TG) were removed by surgical excision. Incubate intact ganglia at 37°C for 20 minutes in papain (25 mg) (Worthington, Lakewood, NJ) in 1 ml Neurobasal A medium (Invitrogen) on a shaker. Remove the papain and incubate for 20 minutes in Neurobasal A medium containing dispase (4.67 mg/ml) and collagenase (4 mg/ml) on a shaker. Mechanically dissociate by triturating, approximately 50 times, with a 1,000-ul pipette. Add dissociated cells to complete Neurobasal A medium (2% B27 supplement Invitrogen, 1% penicillin- streptomycin (PS), NGF 50 ng/ml (Invitrogen). Transferred neurons to be plated on poly-D-lysine- and laminin-coated well. At 24 hours post-plating, remove extracellular debris by gently washing well with Neurobasal A medium. Neuronal cultures can be maintained with complete neuronal medium for up 2-3 weeks by replacing medium weekly, if needed.

2.6 *Analysis of targeted mutagenesis of HSV-1 U_L19*

The target site of the homing endonuclease HSV-1-M5, HSV-1 U_L19, was PCR amplified using UL19 B primers: Forward 5'- GGCCGGCGGAAGTAGTTGAC-3' and Reverse 5'-CACCGACATGGGCAACCTTC-3', with thermocycling conditions of: 94C for 5 min, then 35 cycles (94C for 30 sec, 60 C for 30 sec, 70C for 30 sec), then 70C for 5

min. PCR amplicon sequenced the DNA containing the target region obtained and cloned into the PCR Blunt-TOPO vector using the Zero Blunt TOPO PCR cloning kit (Invitrogen). Target sequence analysis by bacterial colony sequencing was performed by Genewiz, and analysis of mutations was performed using Genius software.

Chapter 3

Delivery and expression of transgenes in sensory neurons of mice

Introduction

Adeno-associated virus (AAV) vectors have become one of the most useful and prevalent gene delivery tools because of their lack of toxicity and low immunogenicity. These viral vectors effectively express transgenes for long periods and in many cell types, including neurons [42-45]. Moreover, such AAV-based vectors have been used in clinical trials and are effective for delivery to the nervous system [46-51]. The most studied AAV vector was based on AAV serotype 2 (AAV2). In fact, multiple researchers have used AAV2 vectors to deliver and express therapeutic genes to the dorsal root ganglia (DRG) [52-57]. Since the development of the AAV2 vector and its successful implementation, other AAV serotypes have been isolated from non-human primates and human sources to be used in research settings as well [58-60].

When used empirically, different AAV serotypes exhibit different cellular tropisms that result in different transduction efficiencies and transgene expression kinetics. For example, direct injection of AAV1 or AAV5 in rodent brains yield a dramatic greater transduction efficiency of neurons in the brain compare to AAV2 [61, 62]. However, AAV8 was reported to show higher levels of transduction when directly injected in the hippocampus compare to AAV1 or AAV5 [63]. Thus, in the central nervous system, the optimal AAV serotype appears to depend on the route of delivery and the target cell type.

To transduce tissues in the peripheral nervous system, direct injection of viral vectors can be accomplish mostly in the dorsal root ganglion (DRG) – particularly, in rodent models of gene delivery. Another method capable of transducing sensory neurons in the DRG is by intrathecal delivery of AAV1 or AAV8 [64, 65]. AAV6 was also found to sufficiently transduce the DRG by injection directly into the sciatic nerve in rats [66]. Although, several groups have reported efficient transduction of DRG neurons, the optimal AAV serotype differed between groups. This is likely due to the delivery route of the AAV vectors. Due to the polarized shape of sensory neurons and the distance between nerve terminals and neuron cell bodies, AAV vectors may encounter a different expression profile of entry receptors on the surface of the cell body compared to the receptors that may be displayed at the surface of nerve terminals. Because of the difference between the anatomical architecture and location of the DRG and the trigeminal ganglion (TG), direct injection into the mouse TG would not be appropriate. Hence, transduction of sensory neurons in the mouse TG must rely on the ability of AAV to enter the nerve terminals that innervate the periphery and be axonally transported in a retrograde manner to the cell bodies of the neurons.

In this study, we determined the dynamics of AAV-mediated gene delivery and transgene expression in sensory neurons in the trigeminal ganglion in mice. We found that AAV serotypes 1, 5, 7, 8, 9 traffic to the trigeminal ganglion from the nerve terminals with similar efficiency after intradermal injection in the whiskerpad. Moreover, we showed that AAV genome levels in the TG remained constant from day 3 to at least day 28 days post inoculation. We established that a vector dose of $5x10^{11}$ AAV vector genomes achieved a transduction efficiency of at least 50% of the neurons in the

TG by whiskerpad injection. Furthermore, significant levels of transgene expression in these transduced neurons were sustained for at least 28 days post inoculation. We found that separate AAVs co-transduced the same neuron, thus enabled delivery of multiple genes at once to the target cell. In addition, we showed that AAV1 co-infect neurons infected with HSV-1, *in vivo*. Our data highlight the parameters to which AAV vectors mediate potential therapeutic gene delivery to sensory neurons of the trigeminal ganglion.

Results

3.1 *AAV1 traffics to the trigeminal ganglion by intradermal injection of the mouse whiskerpad*

Viruses that infect sensory neurons in the trigeminal ganglion, such as HSV-1, can do so by entering the nerve terminals that innervate the ocular region. It has been well established that scarification of the cornea enhances HSV-1 infection of the TG [38]. Since nerve terminals of the trigeminal ganglion also innervate the dermis layer of the whiskerpad in mice, we hypothesized that direct injection of AAV vectors into the dermis of the whiskerpad should lead to efficient viral vector uptake at these nerve terminals. After neuronal entry, via the nerve terminals, vector capsids that contain the expression cassette can be transported to the cell body of the neuron where expression of the transgene is established. To determine the appropriate route of administration of AAV vectors, we compared inoculation of AAV vectors to the cornea or whiskerpad in mice (Figure 2C).

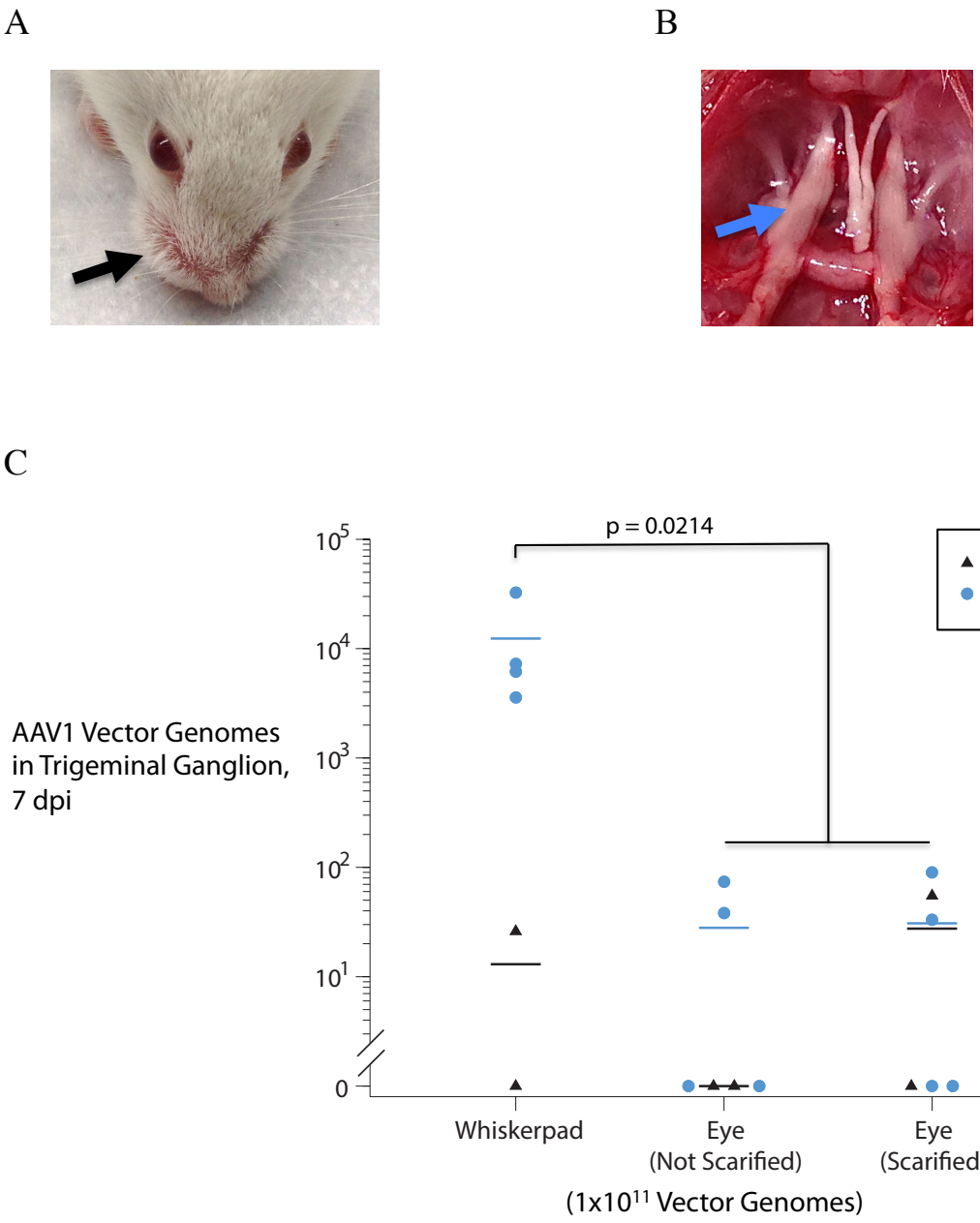

Figure 2. AAV-1 vectors traffic to the trigeminal ganglion after intradermal injection of the mouse whiskerpad
(A) Intradermal injection of the right whiskerpad (black arrow) with 50ul AAV1 vectors (1x10^{11} vector genomes). (B) Mouse trigeminal ganglion (blue arrow). (C) AAV vector genomes in the trigeminal ganglion were quantified by real-time PCR, 7-days post-inoculation in the whiskerpad or eye (non-scarified or scarified cornea). Each triangle or circle represents one trigeminal ganglion. p value = 0.0214 (t-test).

Intradermal injection in the whiskerpad of AAV vectors resulted in an observable bolus at the injection site (Figure 2A) that resumed to normal, 24-hours post inoculation.

Seven days after inoculation of concentrated AAV1 vectors ($1x10^{11}$ vector genomes) in the whiskerpad or in the eye (scarified or non-scarified cornea), real-time PCR of the trigeminal ganglion (Figure 2B and C) showed that AAV vector genomes could readily be detected in the TG following whiskerpad injection, but not via inoculation in the eye. Therefore, intradermal injection of the mouse whiskerpad showed to be an effective route of administration to deliver AAV vectors to the trigeminal ganglion.

3.2 *Effects of AAV serotypes in transduction of neurons in the trigeminal ganglion*

Different AAV serotypes, primarily, represent different surface proteins of the capsid. These differences in capsid surface proteins allow a variety in cellular tropisms. Currently, there are at least ten different AAV serotypes that can be easily constructed. AAV vector-mediated gene delivery to the target cell depends on several specific interactions of the capsid proteins with the target cell. The initial steps include primary recognition and binding of viral vector surface proteins. Then, induction of endocytosis and release from the endosomal compartment follows. Once the entire viral vector particle enters the sensory neuron of the trigeminal ganglion, the capsid still has to be axonally transported via retrograde to the cell body. Here, we tested the ability of AAV serotypes 1, 5, 7, 8, and 9 to enter the nerve terminals of the mouse whiskerpad and be transported to the trigeminal ganglion (Figure 3). We chose to test AAV serotypes 1, 5, 7, 8, 9 because they have been previously demonstrated to successfully transduce various nervous tissues [43-48].

To quantitatively analyze various AAV serotypes with respect to their ability to traffic from the site of inoculation (whiskerpad) to the trigeminal ganglion, we packaged

the same DNA genome flanked by two inverted terminal repeats (ITRs) from AAV2 into capsids of different AAV serotypes. This allowed us to use a specifically designed primer and probe set that amplifies a sequence within the 5' ITR of AAV2 with high specificity. Therefore, all AAV vectors, regardless of serotype, were quantified with the same method.

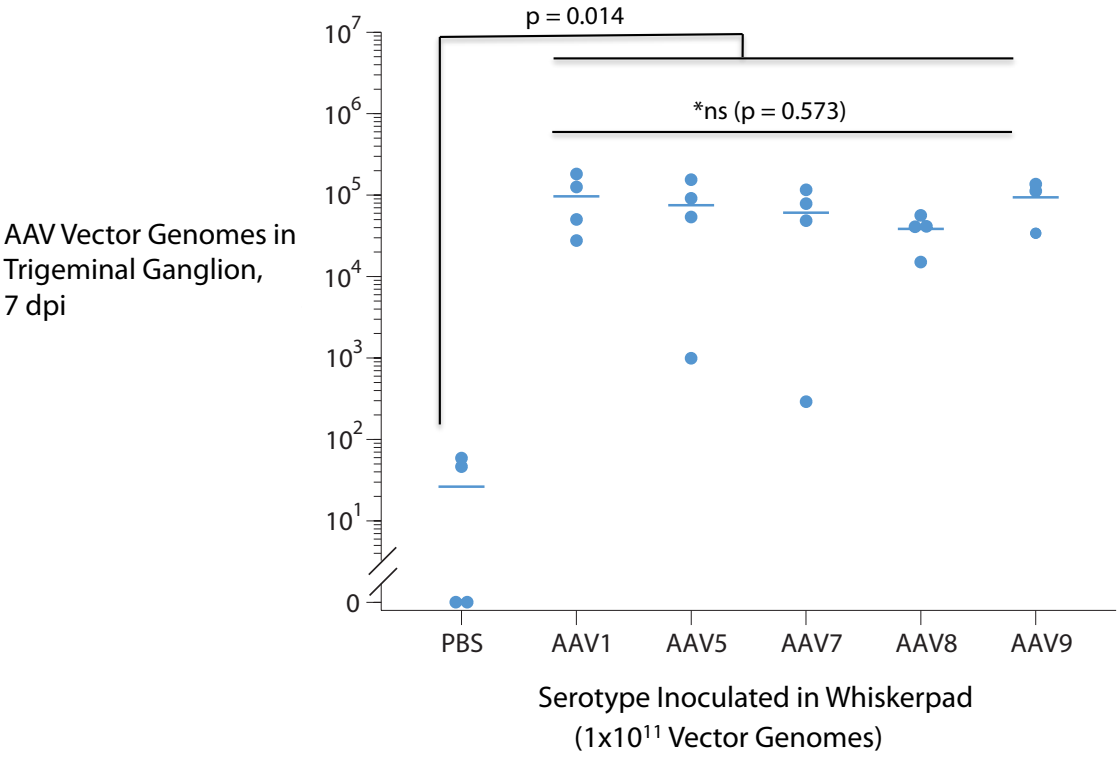

Figure 3. AAV serotypes 1, 5, 7, 8, and 9 traffic to the trigeminal ganglion from the whiskerpad with similar efficiency

Capsids of AAV serotype 1, 5, 7, 8, or 9, packaged with the same vector genome, were intradermally injected in the mouse whiskerpad. Seven-days post-inoculation, AAV vector genomes in the trigeminal ganglion were quantified using real-time PCR. p value = 0.014, *ns (p = 0.573) non-significant; (one-way ANOVA - analysis of variance). Each circle represents one trigeminal ganglion.

A

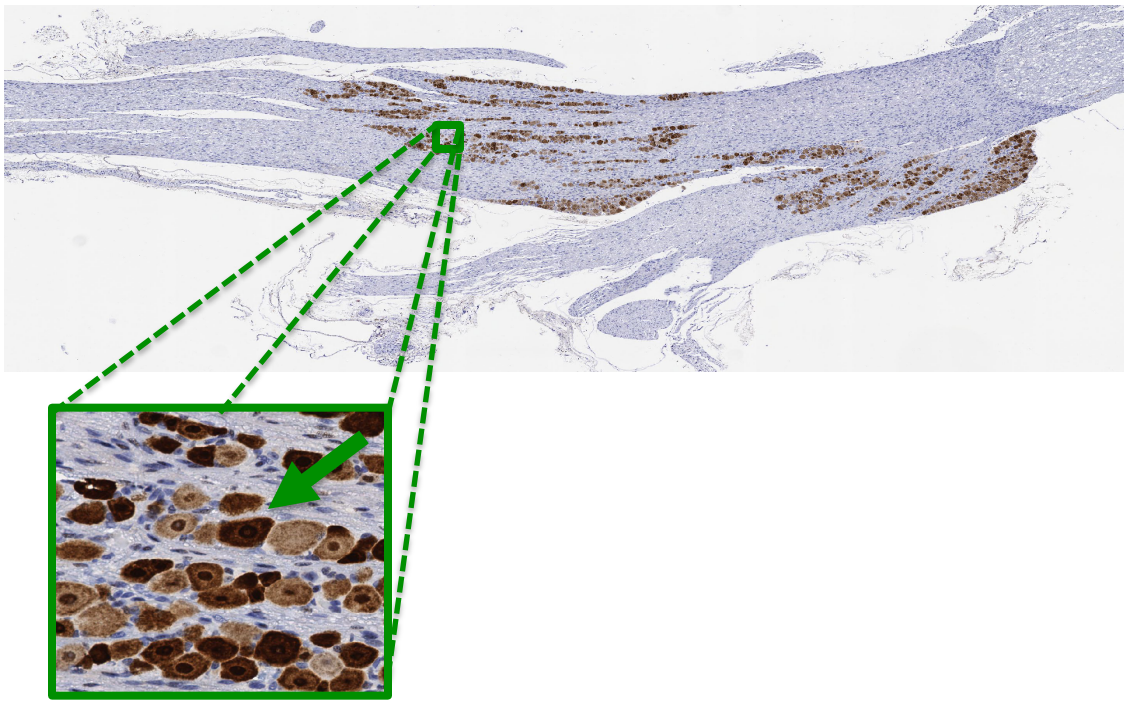

B

Negative control
IHC: hematoxylin

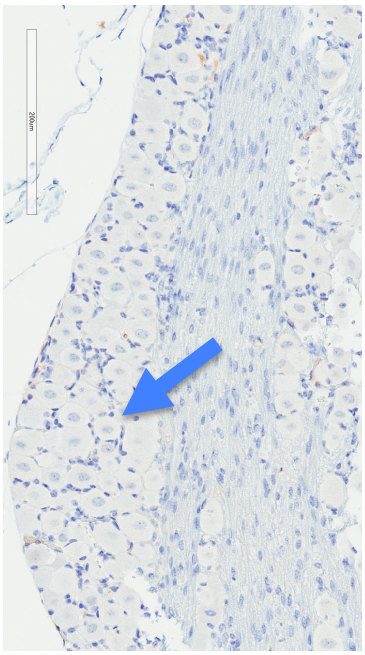

C

Positive control
IHC: anti-NeuN

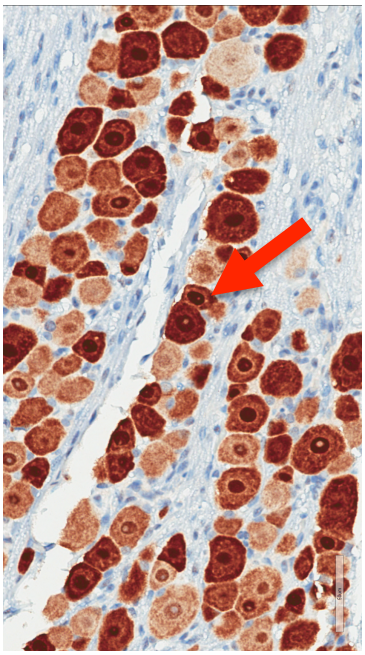

D

AAV8-CMV-mCherry
IHC: anti-mCherry

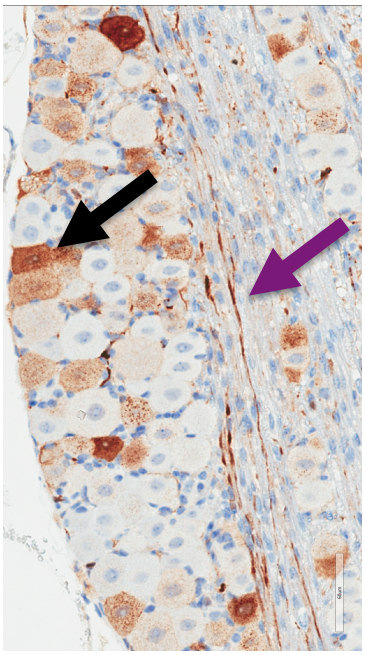

E

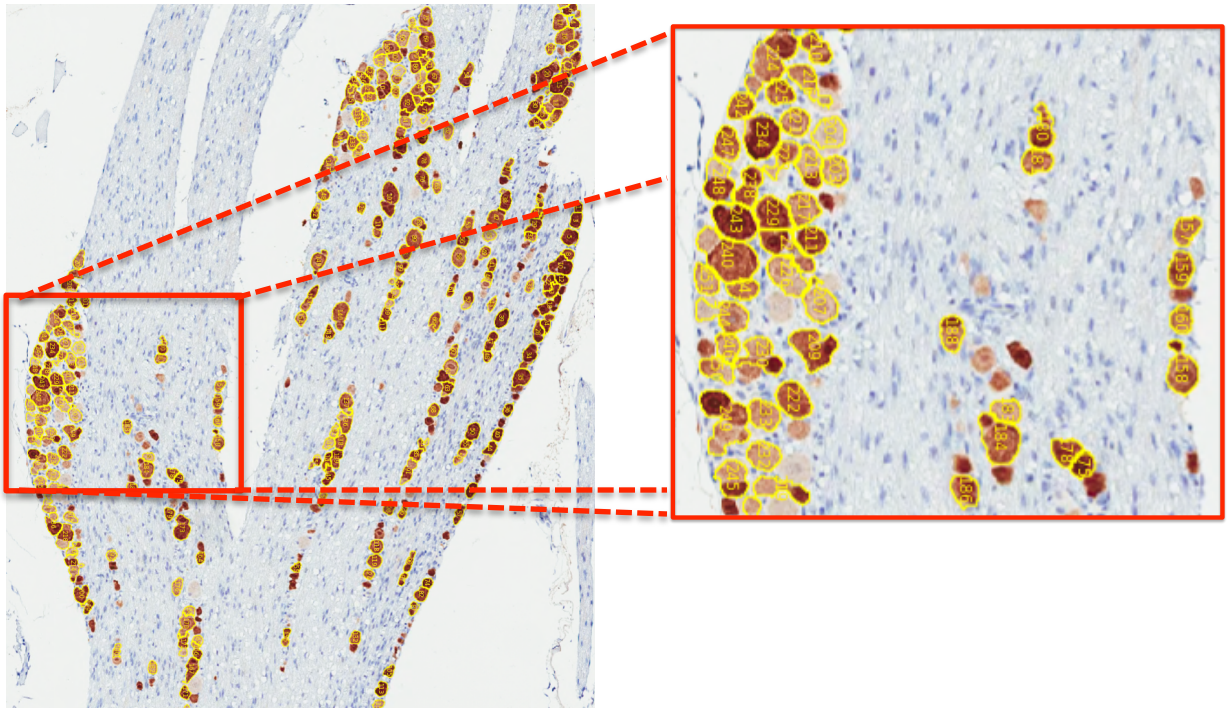

F

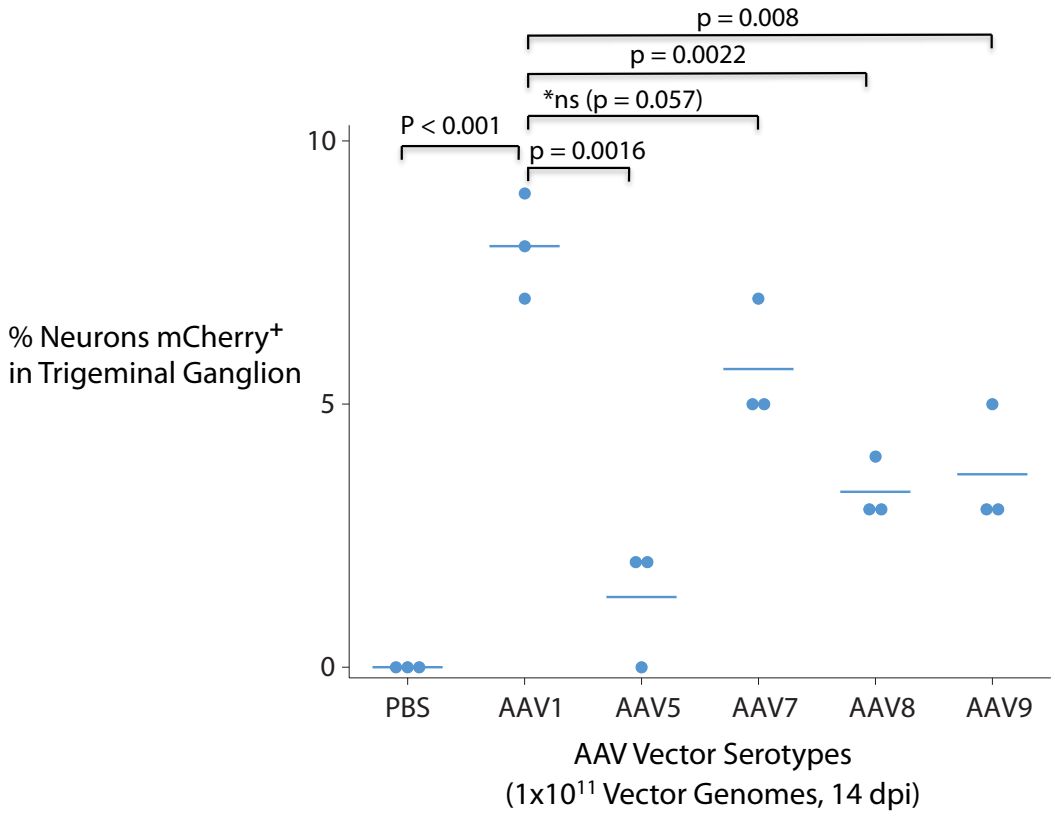
p = 0.008
p = 0.0022
*ns (p = 0.057)
P < 0.001
p = 0.0016
10
5
0
% Neurons mCherry+
in Trigeminal Ganglion
PBS
AAV1
AAV5
AAV7
AAV8
AAV9
AAV Vector Serotypes
(1x10^11 Vector Genomes, 14 dpi)

Figure 4. AAV serotype 1 most efficiently transduce sensory neurons of the trigeminal ganglion
(A) Histology of 4 μM serial section stained with anti-NeuN of the entire trigeminal ganglion from naïve mouse (green arrow = NeuN positive neuron). (B) Histology of hematoxylin stained mouse trigeminal ganglion tissue transduced with AAV1-CMV-mCherry (blue arrow = neuron). (C) Histology of anti-NeuN stained mouse trigeminal ganglion tissue transduced with AAV1-CMV-mCherry (red arrow = NeuN positive neuron). (D) Histology of anti-mCherry stained mouse trigeminal ganglion tissue transduced with AAV-1-CMV-mCherry (black arrow = mCherry positive neuron; purple arrow = mCherry positive axon. (E) Cell Profiler Image Analysis Software used to quantitate mCherry or NeuN positive neurons; each neuron is assigned and catalogued by number associated with its intensity profile. (F) Quantitation of mCherry-expressing neurons after whiskerpad injection of AAV1-CMV-mCherry, 14-days post-inoculation. Total number of neurons per ganglion was quantified with immunohistochemistry for NeuN. p value < 0.0001; p = 0.0016; *ns (p = 0.057); p = 0.0022; p = 0.008; independent two sample t-test. Each circle represents one trigeminal ganglion.

Regardless of serotype, AAV1, 5, 7, 8, and 9, trafficked from the whiskerpad to the trigeminal ganglion with similar efficiency, 7-days post inoculation (Figure 3). Because only nerve terminals of sensory neurons in the trigeminal ganglion innervate the whiskerpad, the likely mode of AAV capsid transport to the cell bodies that are located in the trigeminal ganglion is by retrograde axonal transport. AAV uses several cell surface glycans for binding and entry. Sialic acid is the dominant entry receptor use by AAV1, while AAV5 uses both sialic acid and platelet-derived growth factor receptor to enter susceptible cells [69-71]. The entry receptor or co-receptor for AAV7 and AAV8 are currently unknown. AAV9 binds the cell surface glycan, galactose, to mediate cellular entry [72, 73]. Although it is unclear how the different AAV serotypes we tested gain entry at the nerve terminals of ganglionic neurons, they enter the neurons and traffic to the cell bodies with similar efficiency.

To evaluate transgene expression of transduced neurons in the trigeminal ganglion, we used a semi-automated histological method. We used Cell Profiler Image Analysis software to identified neurons based on cell size, morphology, and positive anti-NeuN or mCherry staining in serial histology sections (Figure 4E). We created a digital map within the histology section by assigning each neuron an identification number.

Therefore, the profile (e.g., cell size, shape, reporter intensity, and location) of the assigned neuron is used to identify that it is a neuron, and determine the relative levels of transgene expression. When we examined for transgene expression from the mCherry reporter, AAV serotype 1 clearly demonstrated to transduce the highest percentage of ganglionic neurons compared to AAV5, 8, or 9 or PBS (Figure 4F). The efficiency of transduction with AAV7 was not statistically different compared to AAV-1.

3.3 *AAV does not induce inflammation in the trigeminal ganglion*

To determine whether AAV vectors induce inflammation in the trigeminal ganglion, we evaluated hematoxylin and eosin stained sections of trigeminal ganglion that have been inoculated with AAV vectors of different serotypes. We injected AAV vectors serotypes 1, 5, 7, 8, or 9 into the whiskerpad of mice at $1x10^{11}$ AAV vector genomes per whiskerpad. Fourteen-days post-inoculation, we could find little evidence of immune infiltrates or tissue damage in the trigeminal ganglion from the AAV serotypes tested (Figure 5A). Presence of AAV vectors in the trigeminal ganglion was confirmed by real-time PCR (see Figure 2). Furthermore, we observe no aberrant alterations in tissue morphology from 3-days post-inoculation up to 28-days post-inoculation of AAV1 (Figure 5B).

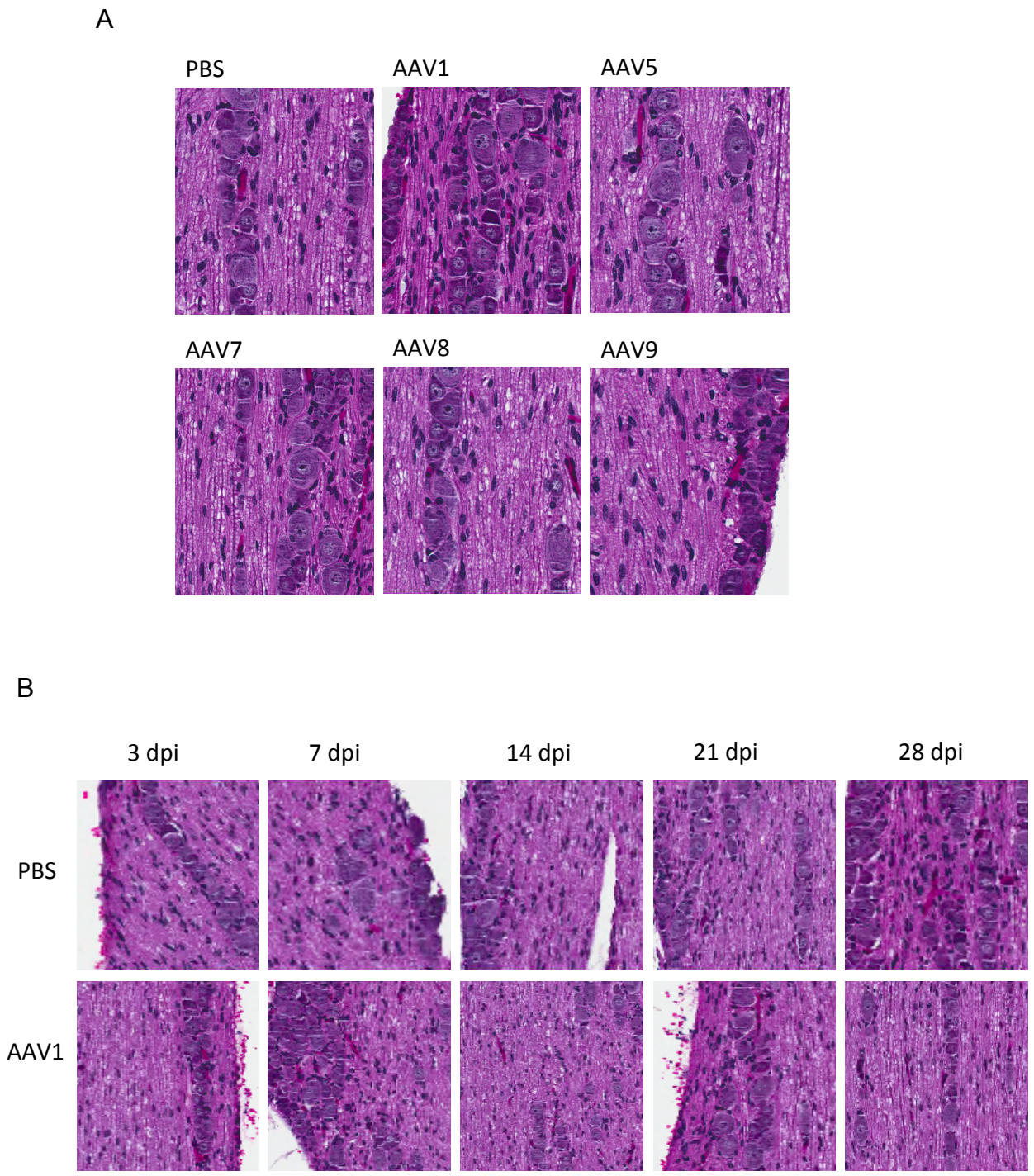

Figure 5. AAV does not induce tissue damage in the trigeminal ganglion
(A) Histology of 4 μM serial section stained with hematoxylin and eosin of the trigeminal ganglion from mice injected with PBS or AAV1, 5, 7, 8, or 9 in the whiskerpad ($1x10^{11}$ AAV vector genomes per whiskerpad. Analysis of H&E stained tissues at 14-days post-inoculation. Representative of three sections per trigeminal ganglion in two mice. (B) Histology of H&E stained mouse trigeminal ganglion tissue transduced with PBS or AAV1 vectors. Analysis of H&E stained tissues at 3, 7, 14, 21, 28-days post-inoculation. Representative of three sections per trigeminal ganglion in two mice.

3.4 *An effective dose of AAV1 is 5x10^{11} vector genomes*

To address how the amount of AAV vectors affected transduction efficiency, we injected increasing doses of AAV1 vector genomes ($5x10^9$, $1x10^{10}$, $5x10^{10}$, $1x10^{11}$, $5x10^{11}$, $1x10^{12}$ vector genomes) in the whiskerpad and quantify the levels of AAV vectors in the TG. We observed that when we increased the amount of AAV vector genomes injected in the whiskerpad, we found more AAV vector genomes in the trigeminal ganglion (Figure 6). The amount of AAV1 vector genomes inoculated in the whiskerpad strongly correlated to the amount AAV1 vector genomes in the trigeminal ganglion at 7-days post-inoculation ($r=0.7331$; $p<0.001$). When we increased the injected dose from $1x10^{11}$ to $5x10^{11}$ AAV vector genomes, we increased the amount of AAV in the trigeminal ganglion from $1x10^4$ to $1x10^6$ AAV vector genomes, respectively. When we increased the injected dose to $1x10^{12}$ AAV vector genomes, we saw no difference in the amount of AAV vector genomes in the trigeminal ganglion compared to an injected dose of $5x10^{11}$ AAV vector genomes. Therefore, in this established mouse model, intradermal injection of $5x10^{11}$ AAV vector genomes in the whiskerpad yielded an effective dose to transduce neurons in the trigeminal ganglion.

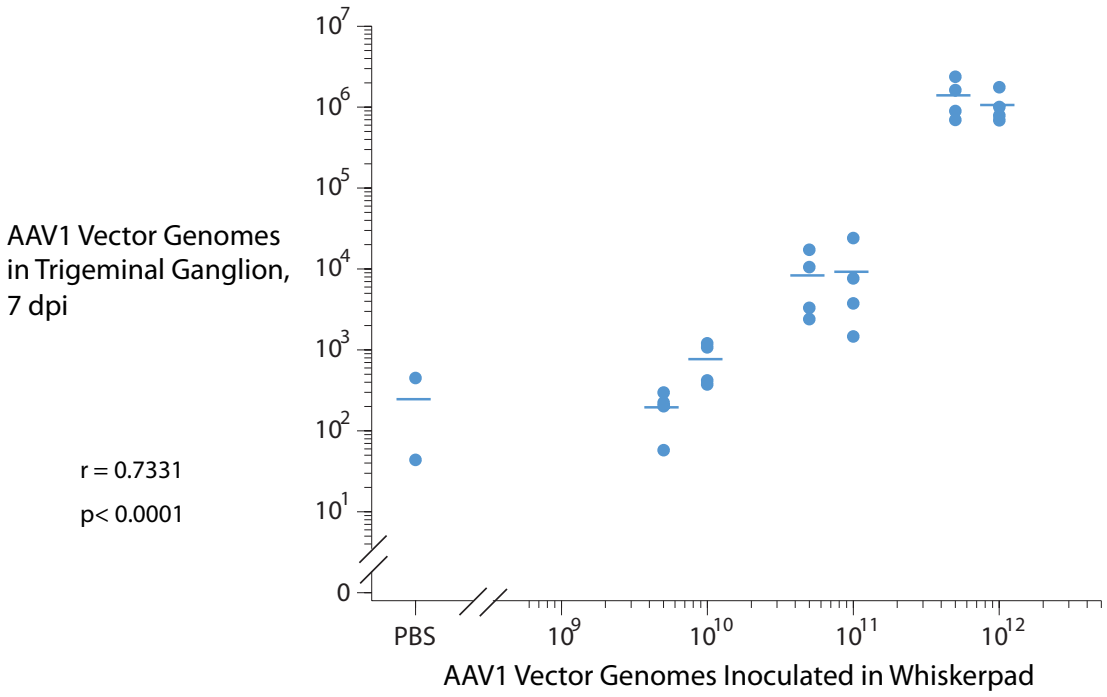

Figure 6. Dose response of AAV vector genomes in the trigeminal ganglion following whiskerpad injection
AAV-1 vectors were intradermally injected in the mouse whiskerpad at $5x10^9$, $1x10^{10}$, $5x10^{10}$, $1x10^{11}$, $5x10^{11}$, or $1x10^{12}$ per whiskerpad. Seven-days post-inoculation, AAV vector genomes in the trigeminal ganglion were quantified using real-time PCR. Correlation coefficient $r = 0.7331$; $p < 0.0001$. Each circle represents one trigeminal ganglion.

3.5 *Levels of AAV genomes in the trigeminal ganglion remain constant, at least to 28 day post inoculation*

To determine the levels of AAV vector genomes in neurons in the trigeminal ganglion over time, we quantified the number of AAV vector genomes at 3, 7, 14, 21, 28-days after whiskerpad injection of AAV1 vectors. We found that when AAV1 trafficked to the trigeminal ganglion, the level of AAV vector genomes in the trigeminal ganglion remained constant from 3 dpi to at least 28 dpi (Figure 7). This finding suggests that AAV vector entry in the nerve terminals occur less than 3 dpi. Furthermore, there

appeared to be no degradation or loss of AAV genomes after AAV vectors traffic to the neuron cell bodies.

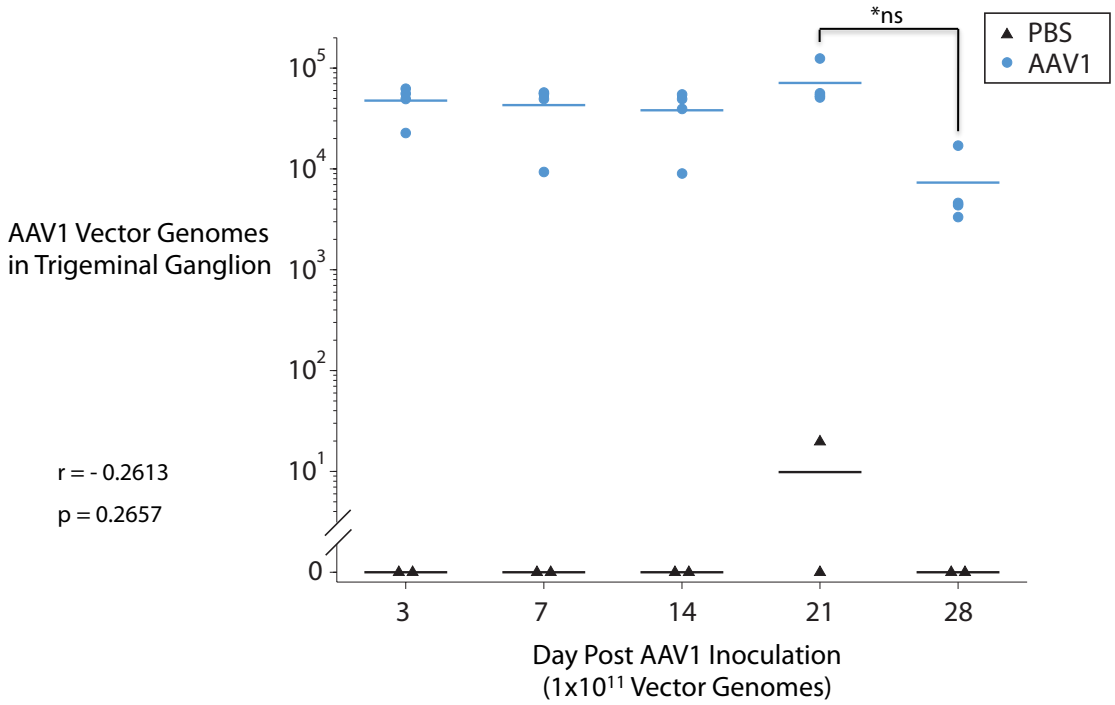

Figure 7. Levels of AAV vector genomes remain constant in the trigeminal ganglion
AAV-1 vectors were intradermally injected in the mouse whiskerpad at $1x10^{11}$ per whiskerpad. At 3, 7, 14, 21, 28 -days post-inoculation, AAV vector genomes in the trigeminal ganglion were quantified using real-time PCR. Correlation coefficient r = -0.2613; *ns (p = 0.2657). Each circle or triangle represents one trigeminal ganglion.

3.6 *AAV-mediated transgene expression increases to 28 day post inoculation*

To evaluate the kinetics of AAV-mediated transduction efficiency, we quantified the proportion of neurons that expressed the delivered transgene over time. Each whiskerpad was intradermally injected with $1x10^{11}$ vector genomes of AAV1-CMV-mCherry. At 3, 7, 14, 21, and 28-days post-inoculation, the percentage of neurons that expressed the mCherry reporter was quantified (Figure 8A). We detected transgene

expression as early as 3 dpi in less than 5% of neurons in the TG. The percentage of neurons that expressed the transgene continued to increase to more than 10% of neurons in the TG by 28 dpi. There is a strong correlation between the increase in the proportion of neurons to express the transgene and the amount of time post inoculation of AAV1 vectors ($r = 0.8942$, $p < 0.0001$). Therefore, it may be likely that the proportion of mCherry-positive neurons continue to increase beyond 28 dpi. We previously demonstrated that the most effective AAV vector dose was $5x10^{11}$ AAV vector genomes (Figure 6). Hence, we tested whether this effective AAV dose resulted in higher transduction efficiency. Indeed, at 4-week post inoculation of $5x10^{11}$ AAV vector genomes, we observed a transduction efficiency of ~50% of neurons in the trigeminal ganglion by whiskerpad injection (Figure 8B).

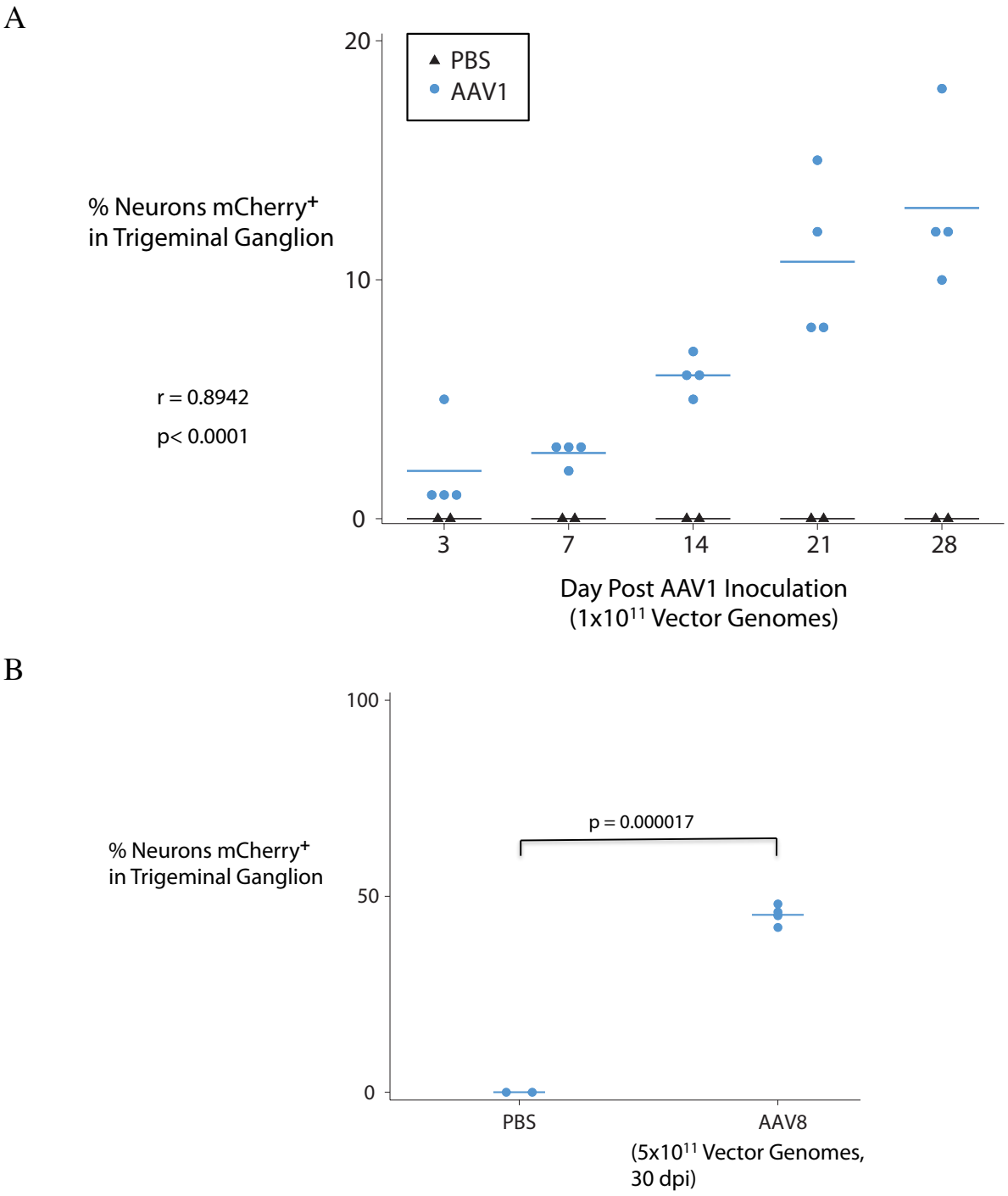

Figure 8. Optimal AAV-mediated transgene expression in the trigeminal ganglion
(A) Quantitation of mCherry-expressing neurons after whiskerpad injection of AAV1-CMV-mCherry at 3, 7, 14, 21, and 28-days post-inoculation. Cell Profiler Image Analysis Software used to quantitate mCherry or NeuN positive neurons; neuron are assigned and catalogued by a number associated with its profile. Correlation coefficient r = 0.8942; $p < 0.0001$. (B) AAV8-CMV-mCherry vectors ($5x10^{11}$ vector genomes) were injected in the whiskerpad. Thirty-days post-inoculation, mCherry reporter expression was quantitated by Cell Profiler software. p = 0.000017; t-test. Each triangle or circle represents one trigeminal ganglion.

3.7 *AAVs co-transduced neurons in the trigeminal ganglion*

AAV vectors used for therapeutic aims, typically, are compose of a single-stranded genome with a capacity of ~4.7 kb in length. Therefore, the transgene in the cassette that is packaged in the AAV capsid has to be less than 4.7 kb. One substantial limitation of the AAV vector is its small packaging capacity. Due to this reason, the delivery of large genes or multiple genes is difficult. Therefore, to overcome this hurdle, we co-transduced neurons with multiple AAVs. This allowed us the ability to co-express multiple transgenes that would be too large to package into one AAV vector genome.

To determine co-transduction of neurons in the trigeminal ganglion, we injected AAV1-CAG-mCherry ($2x10^{11}$ vector genomes) and AAV1-CAG-GFP ($2x10^{11}$ vector genomes) in the mouse whiskerpad and analyzed the proportion of neurons that co-expressed mCherry and GFP by fluorescence microscopy. At 2-days post-explant, 54% of total neurons expressed GFP, 50% of total neurons expressed mCherry, and 38% of total neurons expressed both, GFP and mCherry (Figure 9).

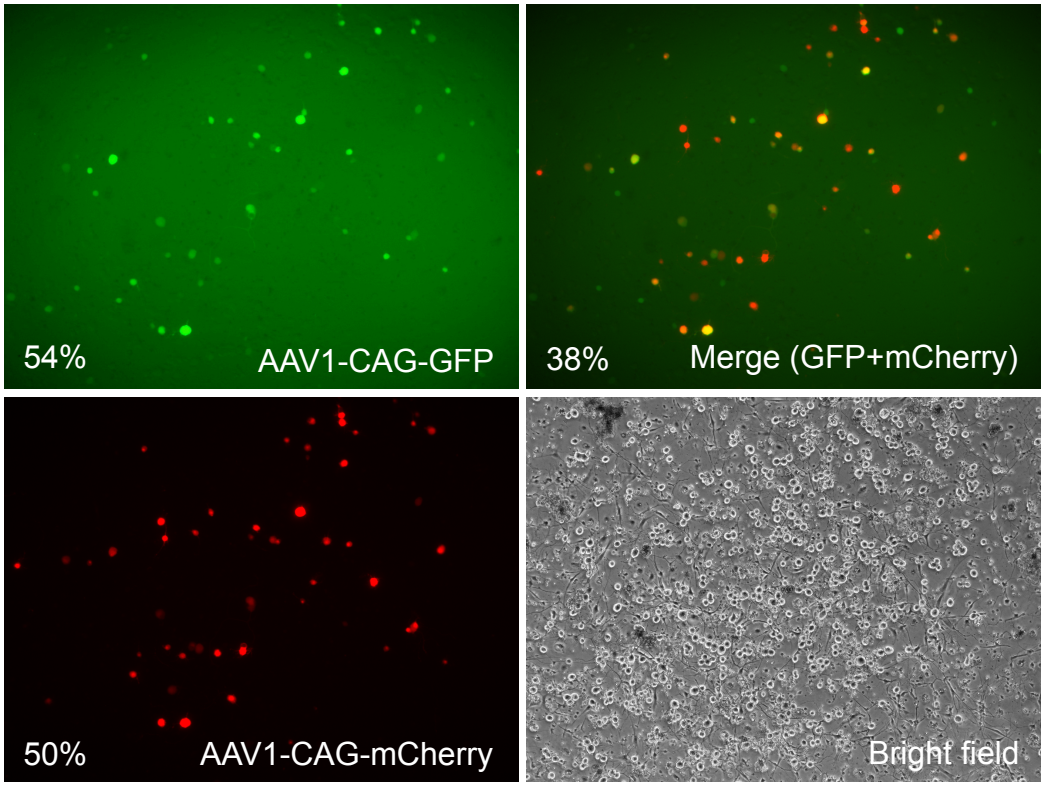

Figure 9. AAVs co-transduced neurons in the trigeminal ganglion
AAV1-CAG-mCherry ($2x10^{11}$ vector genomes) and AAV1-CAG-GFP ($2x10^{11}$ vector genomes) were injected in the mouse whiskerpad at the same time. Twenty-days post-inoculation, trigeminal ganglia were explanted, dissociated, and cultured. Fluorescence images were taken at 48 hours post-explant, and proportion of GFP and mCherry positive neurons were evaluated. 54% of neurons express GFP; 50% of neurons express mCherry; 38% neurons express, both, GFP + mCherry. Representative from one of two mice in experiment.

Discussion

We demonstrated that adeno-associated virus (AAV) vectors can be used for gene delivery to sensory neurons of the trigeminal ganglion in mice. We showed that AAV serotypes 1, 5, 7, 8, 9 trafficked to the trigeminal ganglion with similar efficiency after intradermal injection of the mouse whiskerpad, but AAV1-mediated transgene expression in transduced neurons was highest compared to other AAV serotypes tested. After whiskerpad injection, AAV vectors trafficked to the trigeminal ganglion in just 3 days, and remained at constant levels in the TG at least 28-days post-inoculation. We determined that $5x10^{11}$ AAV vector genomes provided the highest levels of AAV-mediated transgene expression in neurons, *in vivo*. Significantly, we demonstrated that at least 50% of neurons were transduced in the trigeminal ganglion just through whiskerpad injection alone. Moreover, the levels of transgene expression were sustained for at least 28-days post-inoculation. We showed that different AAVs co-transduce neurons, *in vivo*. This allowed us to potentially deliver multiple genes packages in multiple AAVs. Our studies comprehensively revealed the dynamics of gene delivery to neurons in the trigeminal ganglion. This dataset allowed us to choose the optimal conditions to administer a gene therapy approach to treat diseases associated with the trigeminal ganglion.

Consistent with other studies, we observed that individual AAV serotypes differ in their ability to transduce and express transgenes in neurons. Moreover, the region of administration of the AAV vectors also influences whether the viral vector are able to

traffic to the target cell. For sensory neurons of the trigeminal ganglion, viral vector uptake must occur at the nerve terminals. We observed that while all the AAV serotypes can enter the nerve terminals and traffic to the cell bodies with similar efficiency, the level of transgene expression could differ dramatically. AAV1 and AAV7 expressed their transgenes with similar efficiency, whereas AAV5, 8, and 9 were limited in there transgene expression. These results indicated that differences in capsid structures and receptors did not affect receptor-mediated entry at the nerve terminals or capsid-driven retrograde axonal transport to the cell bodies. Thus, it is likely that uncoating of the AAV capsids in the cell bodies may be the rate-limiting step for early and robust transgene expression.

Several studies indicate that AAV vectors generally have the ability to transduce a broad range of neural cell types [62-67]. In our study, we focused on sensory neurons of the mouse trigeminal ganglion. We quantitatively defined the parameters for optimal AAV-mediated gene delivery. When we compared how different AAV serotypes affect transduction efficiencies, we verified transduction based on transgene reporter expression. Expression of the reporter gene could be affected by other factors than just the AAV serotype. Transgene expression levels could also be determined by efficiency of the promoter, as well. One has to consider the tissue context, target cell, and cellular morphology. For example, tissue specific promoters can be use to tune expression levels in the cell. Furthermore, an inducible system of gene control can be implemented. For example, transgene expression under Cre-recombinase dependent vectors could be used in Cre-expressing transgenic mice.

In additional to delivery of therapeutic encoded genes mediated by AAV vectors,

transport of viral vectors within the nervous system can be of interest for axonal tracing studies and projection-specific targeting of neurons. In our study, we primarily observed transduced cell bodies only in the neurons that are likely to have nerve terminals that innervate the region of AAV vector inoculation. Because we used replication defective AAV vectors, synaptic transmission of viral vectors may not be suitable for such studies. It has been reported that injection of AAV5 vectors into the dentate gyrus of the mouse brain led to transduction of excitatory neurons in the lateral entorhinal cortex, not by axonal transport but perhaps by synaptic transfer [74].

We noticed that initial AAV-mediated transgene expression in sensory neurons was relatively slow. We observed a 2-3 week delay in terms of AAV vector entry and detectable levels of reporter expression. It would be useful to compare the kinetics of transgene expression of single-stranded AAV (ssAAV) versus self-complementary AAV (scAAV) vectors in transduce sensory neurons. Because of the double-stranded DNA coding region of the scAAV, it does not require second-strand synthesis as with ssAAV. Thus, given the appropriate AAV serotype and optimal viral vector dose, self-complementary AAV vectors can potentially lead to shorter onset of transgene expression in neurons compared to ssAAV. Such side-by-side comparisons of how the AAV vector genome affects the temporal aspects of transgene expression would be a useful parameter to know in gene delivery design.

Chapter 4

Establishing a model for targeted mutagenesis of HSV-1 infected sensory neurons

Introduction

Most humans are infected with herpes simplex virus type 1 (HSV-1) in childhood or adolescence, and remain latently infected throughout life. HSV-1 enters epithelial cells of the mucosa in the mouth. There, a lytic phase of primary infection develops in infected epithelial cells. Alternatively, viral particles may encounter nerve terminals that innervate the site of primary infection. After HSV-1 enter nerve terminals, viral capsids are translocated via retrograde axonal transport to the neuronal cell bodies. HSV-1 evades antiviral immunity by establishing latency in neurons, a phenomenon in which viral genomes persist as intranuclear episomes for life.

Typically, minor herpetic lesions (cold sores) can result from a productive infection. In other cases, recurrent ocular infections can cause irreversible corneal scarring that may lead to blindness. Recurrent HSV-1 is the leading cause of infectious corneal blindness in the U.S. [20]. In rare cases, encephalitis can ensue when HSV-1 infects the central nervous system (CNS). Although rare, herpes simplex encephalitis is often fatal [21]. Serology and detection of HSV-1 DNA in the trigeminal ganglia (TG) demonstrate that approximately 80% of adults in the world is infected with HSV-1 [21]. Thus, recurrent HSV-1 infections can progress to serious disease, morbidity, and even mortality at any point in the infected person's lifetime.

Current interventions can only suppress HSV-1 replication. To suppress virus replication, pharmacological antivirals are commonly used today. The most common antiviral drugs used to treat HSV-1 infections are nucleoside analogs. Idoxuridine, discovered by Kaufman *et al.* in 1962 was first used to treat HSV eptithelial keratitis [21]. Since then, Acyclovir (ACV), a more advanced derivative of the original nucleoside analog is widely used as topical, intravenous, and oral pills. Other drugs, such as Ganciclovir, foscarnet, cidofovir are also used to treat herpes infections. Additionally, interferons have been tested for therapy as well. Such available drugs work by interfering the ability of the virus to replicate their genome or prevent entry into susceptible cells. Antivirals can decrease the viral load in the infected individual by several orders of magnitude, but residual shedding of virus is exhibited in spite of an aggressive antiviral regimen [88]. Although these drugs can suppress virus replication, they do not prevent viral reactivation and recurrent disease from occurring.

HSV-1 establishes lifelong neuronal latency, which can be easily detected in the trigeminal ganglia (TG). Hill *et al.* (1996) showed that from 174 autopsy samples of human TG, they found that ~90% were detected to have HSV-1 DNA. Moreover, the copy number of HSV-1 genomes had a wide range, from 10 to 3,000 copies per 100ng of host DNA [23]. In the infected neuron, the HSV-1 double-stranded (ds) genome of 152 kb is maintained during latency as circular extrachromosomal episomes as opposed to linear dsDNA during the lytic phase of infection [21].

Our goal is to demonstrate the use of targeted nucleases to impair essential viral genes in HSV-1 infected neurons, *in vivo*. Homing endonuclease (HEs) are natural occurring nucleases that can be engineered to recognize a desired DNA sequence. HEs recognize very long DNA sequences (14-44 bp), which give them exquisite specificity [19]. To repair DNA double-strand breaks (DSBs), homologous recombination (HR) and non-homologous end joining (NHEJ) are

two competing DSB repair mechanisms. Absent of a homologous template, NHEJ is favored. Moreover, NHEJ is the predominant DSB repair pathway in higher eukaryotes [19]. NHEJ is error-prone, and can result in mutations at the repair site caused by insertions or deletions. Under this premise, we employed engineered sequence-specific HEs to mutate essential HSV-1 genes in infected neurons in mice.

To test our target mutagenesis approach, we established a relevant mouse model. Evidence of HSV latency in nervous tissue of small animal models has been established for more than three decades. The murine model for HSV-1 infection and latency is an attractive model because it recapitulates most aspects of HSV-1 life cycle. HSV-1 can establish infection at peripheral sites in mice similar to humans, and importantly HSV-1 establishes latency in sensory neurons in the trigeminal ganglia (TG) of the mouse [33]. Therefore, we aimed to exploit the mouse model of HSV-1 infection to test our approach of targeted mutagenesis of viral genomes in infected neurons.

Results

4.1 *Quantification of HSV-1 load in trigeminal ganglion: ocular vs whiskerpad inoculation and acute vs latent infection*

The ocular infection model of HSV-1 has been well established in the field, and can recapitulate most aspects of the viral life cycle. We demonstrated that AAV-mediated gene delivery and transgene expression in the mouse trigeminal ganglion (TG) is most efficient by intradermal injection of the whiskerpad (Figure 2 and Figure 8). To determine the optimal route of HSV-1 infection in the mouse TG, we compared HSV-1 inoculation via the ocular route versus whiskerpad injection. Mice were inoculated with HSV-1 KOS ($5x10^6$ PFU) either in the scarified cornea or whiskerpad. At 7 or 21-days post-inoculation, the amount of HSV-1 genomes per ganglion was determined by digital droplet PCR. In the mouse model, 7-dpi represented the peak of the lytic cycle of HSV-1 infection. In contrast, at 21-dpi, HSV-1 latent infection in neurons of the TG has been established. At 7-dpi, mice inoculated with HSV-1 KOS via the ocular route showed a viral load of ~$5x10^5$ HSV-1 DNA copies per ganglion, compared to a viral load of ~$1x10^4$ HSV-1 DNA copies per ganglion when HSV-1 was injected in the whiskerpad (Figure 10). At viral latency or 21-dpi, the differences in viral loads in the TG from ocular versus whiskerpad injection was not significant (Figure 10).

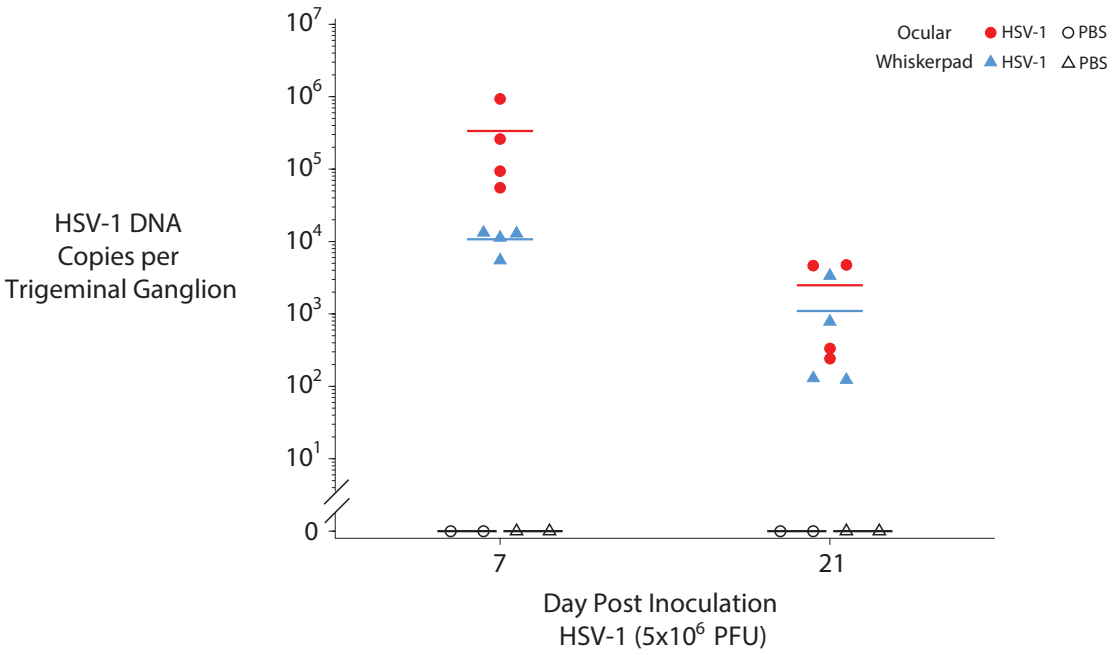

Figure 10. Quantitation of HSV-1 DNA in the trigeminal ganglion
HSV-1 KOS ($5x10^6$ PFU) was inoculated to the scarified cornea or by intradermal injection in the whiskerpad. At 7 or 21-days post-inoculation, copies HSV-1 DNA in the trigeminal ganglion were quantified using droplet digital PCR. Each circle or triangle represents one trigeminal ganglion.

4.2 *Establishment of HSV-1 latency and viral reactivation*

To test targeted mutagenesis of HSV-1 genomes in infected neurons, we showed that latent HSV-1 reactivate to produce infectious virus. Mice were inoculated with $2x10^5$ PFU HSV-1 in the left scarified cornea. At 4-week post-inoculation, the left eye appeared normal and latency was presumed established in the trigeminal ganglion. To assess the ability of latently infected neurons to reactivate, trigeminal ganglia from latently infected mice were excised and co-cultured with susceptible indicator cells. Sample supernatant from co-cultures were assayed daily to determine infectious virus by cytopathic effects on indicator Vero cells. At 3-day post-explant, co-cultures of the ipsilateral trigeminal ganglion demonstrated viral reactivation as evident in cell lysis as a result of infectious HSV-1 replication (Figure 11). In contrast, co-

cultures of the contralateral trigeminal ganglion with indicator cells show less than 30% infectious virus production. Infectious virus from the contralateral TG is likely due to the transfer of HSV-1 from the ipsilateral eye to the contralateral eye during primary infection.

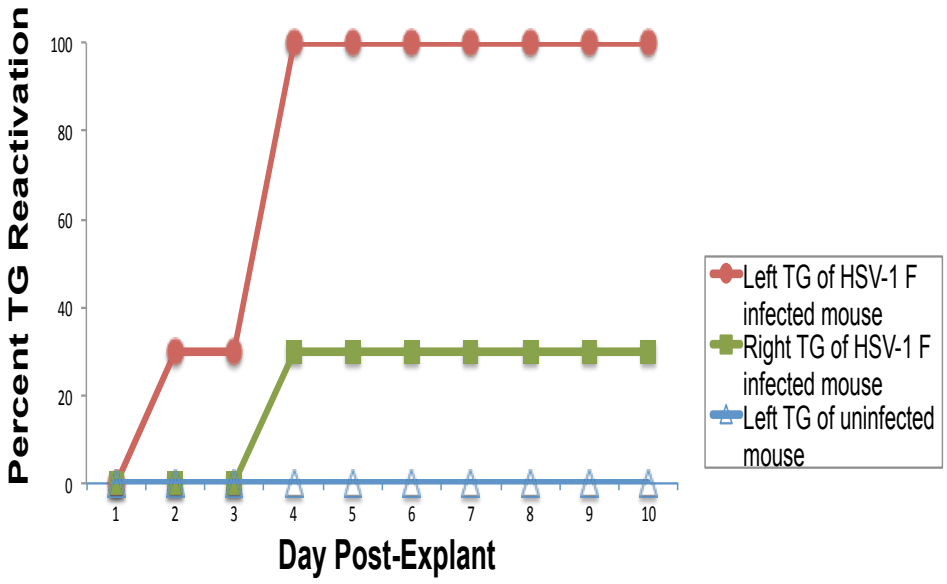

Figure 11. Establishment of HSV-1 latency and reactivation of the trigeminal ganglion in mice
HSV-1 ($2x10^5$ PFU) was inoculated to the left scarified cornea. At 4-weeks post-inoculation, trigeminal ganglia was explanted and co-cultured with Vero cells. Supernatant from explanted co-culture were assayed daily on indicator cells to detect infectious virus. Time points represent cumulative percentage of trigeminal ganglia that reactivated latent HSV-1. Experiment representative of 3 mice per group.

4.3 *Co-infection of AAV1 and HSV-1 in sensory neurons*

One critical step in establishing a model for targeted mutagenesis of HSV-1 in infected sensory neurons is to deliver the gene-encoded therapeutic nuclease to HSV-1 infected neurons in the trigeminal ganglion. In this context, we evaluated whether AAV1 vectors and HSV-1 can co-infect sensory neurons, *in vivo*. After we injected AAV1-CAG-mCherry vectors ($1x10^{11}$ vector genomes) in the whiskerpad of mice, we waited 7-days before inoculating the ipsilateral whiskerpad with HSV-1-CMV-GFP ($1x10^{6}$ PFU). At 5-days post-inoculation with HSV-1, we explanted the trigeminal ganglion to analyze for reporter expression, *in vitro,* by fluorescence imaging. We found that greater than 60% of neurons were co-infected with AAV1 and HSV-1, *in vivo* (Figure 12). As shown in Figure 4, an inoculum dose of $5x10^{11}$ AAV vector genomes resulted in two orders of magnitude increase of AAV vector genomes in the trigeminal ganglion compared to an inoculum dose of $1x\ 10^{11}$ AAV vector genomes. Therefore, it is likely that inoculation of a higher AAV vector dose, $5x10^{11}$ vector genomes, in the whiskerpad may lead to an increased co-infection rate of AAV1 and HSV-1.

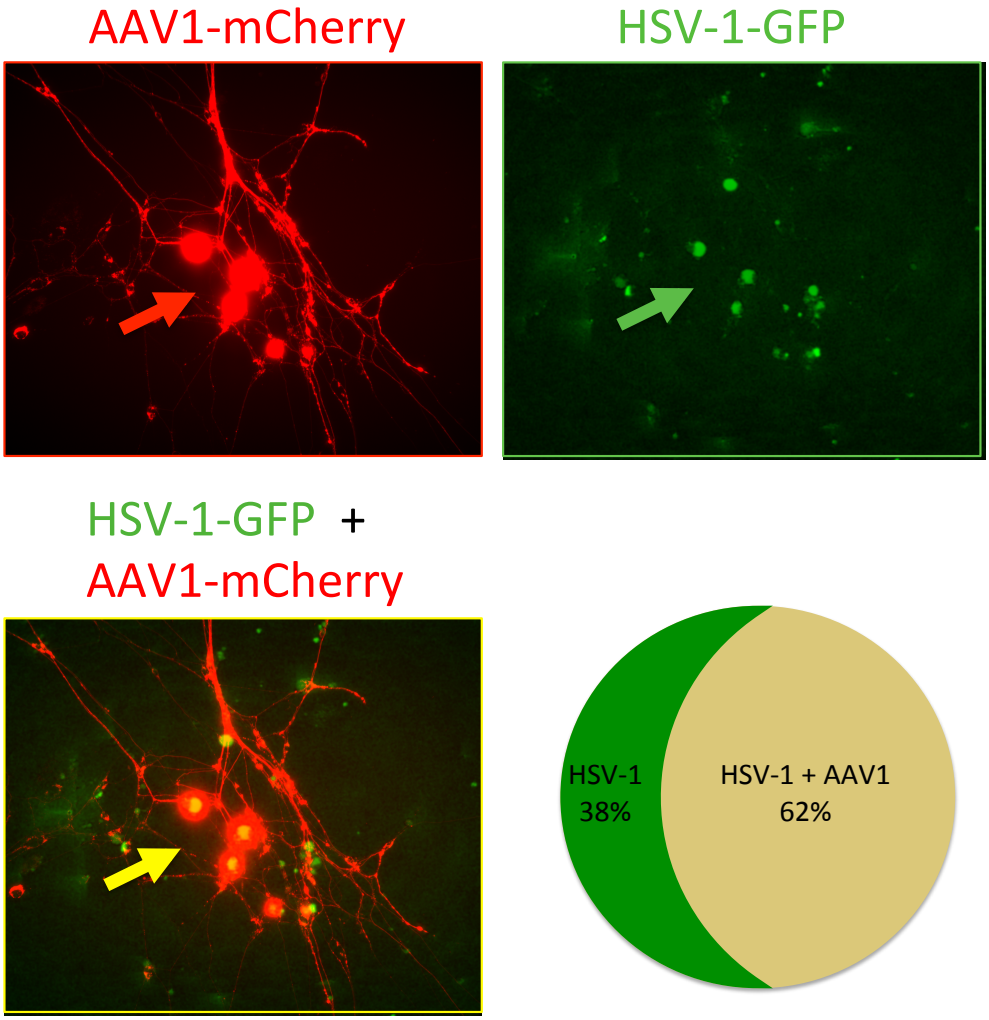

Figure 12. AAV1 and HSV-1 co-infect sensory neurons in the trigeminal ganglion *in vivo*
AAV1-CAG-mCherry vectors ($1x10^{11}$ vector genomes per whiskerpad) were intradermally injected in the mouse whiskerpad. Seven-days post-inoculation of AAV1, HSV-1-CMV-GFP ($1x10^{6}$ PFU per whiskerpad) was inoculated in the ipsilateral whiskerpad. Five-days post HSV-1 infection, trigeminal ganglia were explanted and cultured with 300 uM acyclovir. Fluorescence imaging was performed 14-days in culture. Experiment representative of 3 mice.

4.4 *Treatment of HSV-1 infected mice with engineered homing endonucleases*

To optimize efficiency of targeted mutagenesis of HSV-1 genomes in infected sensory neurons, we used an HSV-1-specific homing endonuclease, HSV-1 M5 (HE M5). This nuclease recognizes a single 24 base pair target sequence in the HSV-1 genome located at the 3' end of U_L19 gene [90]. The U_L19 gene encodes for the major capsid protein, VP5, which is essential for the survival and infectivity of HSV-1. AAV1-CMV-HE-M5 vectors ($2x10^{11}$ vector genomes) were intradermally injected in the mouse whiskerpad. To allow sufficient time for HE-M5 to be expressed in transduced neurons, we waited 2 weeks before we established an HSV-1 infection in the trigeminal ganglion. Because the viral load of HSV-1 is highest during the acute phase of infection (Figure 10), we analyzed for frequency of mutation after 5-days post-infection of HSV-1. We observed mutagenesis of about 1% at the U_L19 target site (Figure 13B). Here, we showed the first observation of targeted mutagenesis of HSV-1 genomes in infected neurons, *in vivo*.

A

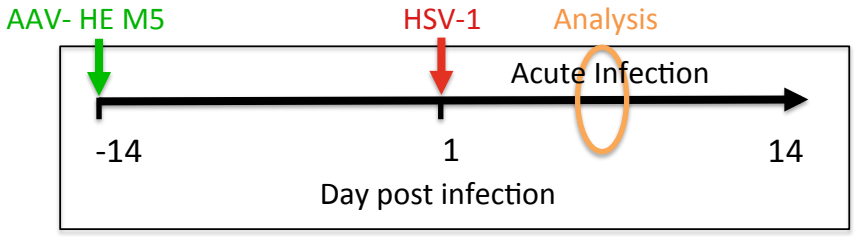

B

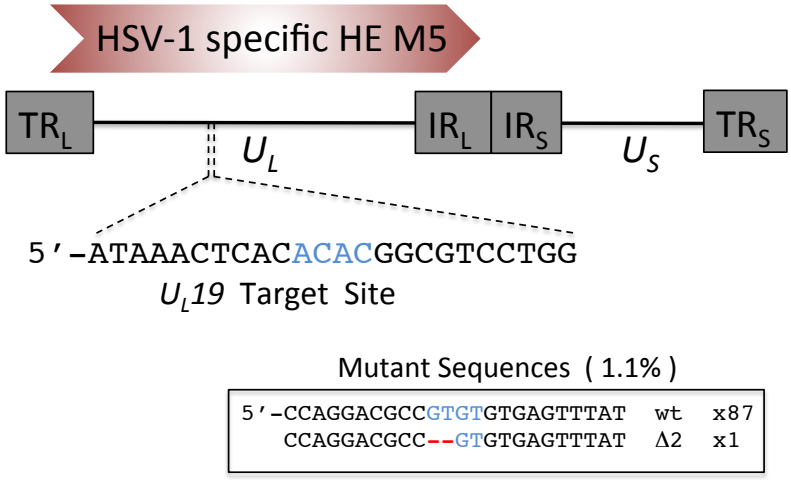

Figure 13. ***In vivo*** **targeted mutagenesis of HSV-1 in infected neurons in the trigeminal ganglion**
(A) Timeline of HE-M5 treatment, HSV-1 infection, and sequence analysis. AAV1-CMV-HE-M5 vectors ($2x10^{11}$ vector genomes per whiskerpad) were intradermally injected in the mouse whiskerpad. Fourteen-days post-inoculation of AAV1-CMV-HE-M5 vectors, HSV-1 ($2x10^5$ PFU) infection of the ipsilateral trigeminal ganglion was established. Five-days post HSV-1 infection, trigeminal ganglia were explanted and amplicon sequencing of HSV-1 U_L19 was performed. (B) A total of 88 amplicons were sequence resulting in 1% mutation rate of two base pair deletion in the HSV-1 U_L19 target site.

Discussion

We presented evidence that adeno-associated virus (AAV) vectors can deliver gene encoded therapeutic nucleases to neurons in the trigeminal ganglion in a mouse model. Furthermore, we could employ engineered homing endonucleases to test targeted mutagenesis of HSV-1 infected neurons, *in vivo*. Specifically, we showed that HSV-1 establishes infection in the trigeminal ganglion by the traditional ocular route of infection or by intradermal injection of the mouse whiskerpad. Moreover, we demonstrated that after establishment of latent infection in the mouse trigeminal ganglion, latent HSV-1 reactivated by explant of the infected trigeminal ganglion. We showed that AAV1 and HSV-1 co-infected sensory neurons in the trigeminal ganglion, thus allowing AAV-mediated gene encoded nucleases to interact with HSV-1 genomes in co-infected neurons. Significantly, we showed targeted mutagenesis of HSV-1 genomes in neurons, *in vivo*.

The goal of this mouse model was to provide proof-of-concept that HSV-1- specific nucleases can promote mutagenesis of HSV-1 genomes in infected sensory neurons in the trigeminal ganglion. This viral gene disruption approach can further be tested in latent HSV-1 infected neurons. During HSV-1 latency, viral DNA genomes are maintained from 1 to ~50 copies per latently infected neuron. In this neuronal reservoir, latent HSV-1 produces no viral proteins, therefore limiting host immunity to infected neurons. Under certain conditions, presumably from stress or other factors, viral reactivation re-establishes productive infection at the original site of infection to cause disease and likely transmission to hosts. By disrupting the latent HSV-1 genome, we may inhibit disease and transmission.

Currently, there are several drugs used to treat HSV-1 infection, mainly by inhibiting viral DNA synthesis. But, such drugs have little effect on latent HSV-1. Because the latent viral reservoir of HSV-1 principally is limited to the trigeminal ganglion, the established mouse model of HSV-1 infection in the cornea or whiskerpad can be utilize to test this directed viral gene disruption approach in relatively low copy numbers of latent HSV-1 genomes in infected neurons. Importantly, we showed that AAV1-mediated gene delivery efficiently transduced a significant percentage of neurons in the trigeminal ganglion.

Use of specific endonucleases for targeted gene disruption relies on error-prone cellular DNA repair of NHEJ. We have shown that exposure of engineered homing endonucleases to HSV-1 infected neurons resulted in detectable mutations within the target site of the HSV-1 genome. Induction of the HE-M5-mediated double-stranded DNA break in the U_L19 target site leaves 3'-overhangs. Therefore, we could increase the frequency of mutation of HSV-1 in infected neurons when we co-express a 3' to 5' exonuclease such as Trex2. Degradation of 3'-overhangs induced by HE-M5 cleavage before DNA ligation of the DSB would likely increase the frequency of mutagenesis within HSV-1 *U_L19*.

Chapter 5

Future Directions

We quantitatively described the dynamics of therapeutic gene delivery to neurons in the trigeminal ganglion, and demonstrated *in vivo* targeted mutagenesis of HSV-1 infected neurons in mice. In humans, and in mouse models of HSV-1 infection, HSV-1 latent viral genomes are found in only a small fraction of sensory neurons in the trigeminal ganglion [21, 41]. Moreover, the number of viral genomes per neuron correlates with the rate of reactivation in mouse models of HSV-1 latency [40, 41]. Therefore, specifically disrupting enough latent HSV-1 genomes may lead to reduction or inhibition of viral reactivation and recurrent disease. However, we need to determine the frequency of viral gene disruption in latently HSV-1 infected neurons that is required to sufficiently impede virus reactivation to a significant level.

In this study, we tested one class of nucleases that was engineered to induce a double-stranded break (DSB) within the HSV-1 U_L19 open reading frame. Currently, there are four major classes of nucleases that can be design to cut desired target sites: homing endonucleases (HEs), zinc finger nucleases (ZFNs), TAL effector nucleases (TALENs), and RNA-guided CRISPR/CRISPR-associated system (Cas) nucleases. We used HEs because of their small size, thus facilitating AAV vectorization. Importantly, HEs can recognize DNA sequences of 14-44 base pairs (bp). This makes HEs highly specific for their target site, which potentially can result in reduce levels of cellular toxicity.

Going forward, it would be attractive to utilize other nuclease platforms to disrupt latent HSV-1, *in vivo*. ZFNs are able to recognize many 3 bp DNA sequences, but because they function in a modular fashion, they can be arrayed to form a larger protein that can bind DNA sequences up to 18 bp in length [75, 76]. ZFNs bind to their DNA target site, but they are typically fused to a non-specific DNA endonuclease such as FokI to promote DSBs at the bound target site. Although, ZFNs have been shown to inhibit DNA virus replication [75, 76], they are less specific then desired.

Transcription activator like endonucleases (TALENs) were developed based upon a DNA binding protein found in the plant bacterium Xanthomonas. TALENs are also modular, thus they can be arrayed to recognize a desired target site [77]. Similarly to ZFNs, TALENs are engineered such that the DNA binding domains must be fuse to an endonuclease such as FokI. TALENs can be designed to recognize a target sequence of 16-32 bp [78], thus making them relatively specific. TALENs are very large, hence for our use, AAV-mediated delivery of gene encoded TALENs would not be feasible due to the packaging capacity of AAV. Furthermore, TALENs are difficult to engineer.

In the last two years, the CRISPR/Cas based system of gene editing has risen to enormous popularity and usefulness. Clustered regularly interspaced short palindromic repeats (CRISPR) loci are found in a wide range of bacteria and thought to behave as an adaptive-immunity-like system for invading bacteriophage [79]. The relative simplicity of the type II CRISPR nuclease, along with the engineered synthetic single guide RNA (sgRNA) has enabled specific gene editing in mammalian cells [80, 81]. Thus, utilizing a wild type Cas9 and a specific sgRNA, a DSB may be induced at a desired target site such

as an essential HSV-1 gene. Following error-prone repair, mutations within the target site can be promoted.

Gene delivery dynamics demonstrated in this study are directly applicable to test the CRISPR/Cas-based approach to disable HSV-1 in infected neurons of the trigeminal ganglion (TG). In this study, we have shown that AAV vectors transduce at least 50% of total neurons in the TG, by just whiskerpad injection alone. The transduction efficiency would likely be much higher if we only accounted for the neurons in the TG that could only be accessible by whiskerpad injection. This would allow us to potentially target the majority of latent HSV-1 genomes in the mouse model of whiskerpad infection. Similar to testing engineered homing endonucleases, it is critical to efficiently deliver gene-encoded components of the CRISPR/Cas system to infected neurons, *in vivo*. AAV vectors can also be utilized, but packaging capacity must be considered. Because the size of the Cas9 gene, along with the nuclear localization signal, promoters, and sgRNA sequences occupy more than the packaging capacity of one AAV vector, we would have to package these components into two AAV vectors. This means that effective co-transduction of AAVs in neurons must be accomplished. In this study, we have shown that ~40% of neurons are co-transduced, with just $2x10^{11}$ AAV vector genomes. The level of AAV vector co-transduction would likely be much higher at the more optimal AAV vector dose of $5x10^{11}$ AAV vector genomes per site of injection.

Although detailed in this study are the parameters to deliver gene-encoded therapeutic nucleases to sensory neurons in the trigeminal ganglion, we must also consider the accessibility of the target site in the latent viral genome by the nuclease in the HSV-1 infected neuron. Following neuronal nuclear entry, the viral genome circularizes and is assemble with histones [21, 83]. Post-translational modification (PTMs) of the histones associated with the viral

genome is believed to mediate epigenetic control of viral gene expression rather than direct modification of the virus DNA by methylation [82-84]. More specifically, during productive infection, the viral genome exhibits a euchromatin form due to the PTMs of histones at position H3K9 (histone 3 lysine 9) and H3K14 [83, 86]. During lytic infection modifications to the euchromatin such as acetylation of H3K9 and H3K14 are enriched on lytic gene promoters, e.g., promoters of immediate early (IE) genes [86]. Moreover, repressive histone modifications such as methylation of H3K9 are less enriched [85-87]. In contrast, during neuronal latency histones presenting acetylated H3K9 and H3K14 are enriched at the promoter of the actively transcribed LAT region while less abundant at the promoter region of the IE gene such as ICP0 or viral DNA polymerase gene [36, 87]. Such epigenetic regulation of the latent HSV-1 genome is of notable importance relating to targeted mutagenesis using site-specific nucleases, and must be appropriately addressed. In other words, the desired target sites of the HSV-1 episomes in latently infected neurons may not all be accessible to nuclease cleavage. The viral genome may be associated with nucleoprotein complexes that inhibit access of the target site for mutagenesis. These nucleoproteins may influence the episome structure so that it is in a compact or "closed" conformation, inaccessible to targeted nucleases. In addition to association of nucleoproteins, the fact that HSV-1 episomes are closed circular dsDNA genomes is more likely to be coiled thus limiting the double-stranded break DNA repair machinery. To address this, we may use chromatin modifiers such as sodium butyrate (NaBut), Trichostatin (TSA), or suberoylanilide hydroxamic acid (SAHA) to promote accessibility of target sites.

In this study, we have shown that AAV vectors do not induce obvious morphological alterations to the trigeminal ganglion by H&E staining of histology sections. But, potential toxicity due to specific therapeutic endonuclease expression in HSV-1 latently infected sensory

neurons will have to be assessed. Animal studies and observations in humans suggest that a strong cell-mediated immune response is prohibited in neurons due to their low levels of MHC Class I expression [21]. The fact that HSV-1 latently infected neurons can persist for life demonstrates that infected neurons can evade a proficient CTL response. However, recent studies show that CD8 T cells do infiltrate infected ganglia, particularly during viral reactivation [88, 89]. Further analysis of cellular toxicity, by evaluating levels of apoptosis, can demonstrate early levels of neuronal toxicity. One can examine apoptosis by assaying intracellular levels of Caspase 3 and cell surface Annexin V upon exposure to nuclease activity. Affected neurons may undergo necrosis, which can be detected by propidium iodide staining. Moreover, morphological changes of dendrite formation and cell body alterations due to toxicity can be easily observed by microscopy, *in vitro*. Additionally, off-target cleavage effects can be assessed by examining treated neurons for gamma-H2AX foci, which is an indicator of the cellular response to double-stranded breaks.

In this study, we tested therapeutic nucleases to treat HSV-1 infection in neurons. This approach for HSV-1 can also be applied to treat HSV-2 and Varicella zoster virus (VZV) latent infections. After primary infection, VZV establishes lifelong latency in sensory neurons with similar frequencies of latently infected cells and viral copy number to HSV-1 [21]. VZV can also reactivate to cause zoster (shingles) and often post-herpetic neuralgia, which can be debilitating. Therefore, AAV-mediated delivery of therapeutic nucleases can be employed to potentially disrupt latent HSV-2 and VZV infections, as well.

Bibliography

1. G. Hsich, M. Sena-Estevas, X.O. Breakefield. Critical issues in gene therapy for neurologic disease. Hum. Gene Ther. 13 (2002) 579–604.
2. W.T. Hermens, J. Verhaagen. Viral vectors, tools for gene transfer in the nervous system. Prog. Neurobiol. 55 (1998) 399– 432.
3. Tratschin, J. D., West, M. H. P., Sandbank, T., and Carter, B. J. (1984). A human parvovirus, adeno-associated virus as a eukaryotic vector: transient expression and encapsidation of the prokaryotic gene for chloramphenicol acetyl transferase. Mol. Cell. Biol. 4: 2072 – 2081.
4. Hermonat, P. L., and Muzyczka, N. (1984). Use of adeno-associated virus as a mammalian cDNA cloning vector: transduction of neomycin resistance into mammalian tissue culture cells. Proc. Natl. Acad. Sci. USA 81: 6466 – 6470.
5. Flotte, T. R., et al. (1996). A phase I study of an adeno-associated virus CFTR gene vector in adult CF patients with mild lung disease. Hum. Gene Ther. 7: 1145 – 1159.
6. T.J. McCown, X. Xiao, J. Li, G.R. Breese, R.J. Samulski. Differential and persistent expression patterns of CNS gene transfer by an adeno-associated virus (AAV) vector. Brain Res. 713 (1996) 99–107.
7. A.L. Peel, S. Zolotukhin, G.W. Schrimsher, N. Muzyczka, P.J. Reier. Efficient transduction of green fluorescent protein in spinal cord neurons using adeno-associated virus vectors containing cell type-specific promoters. Gene Ther. 4 (1997) 16–24.

8. J.S. Bartlett, R.J. Samulski, T.J. McCown. Selective and rapid uptake of adeno-associated virus type 2 in brain. Hum. Gene Ther. 9 (1998) 1181–1186.
9. Y.J. Hernandez, J. Wang, W.G. Kearns, S. Loiler, A. Poirier, T.R. Flotte. Latent adeno-associated virus infection elicits humoral but not cell-mediated immune responses in a nonhuman primate model. J. Virol. 73 (1999) 8549–8558.
10. W.C. Manning, S. Zhou, M.P. Bland, J.A. Escobedo, V. Dwarki. Transient immunosuppression allows transgene expression following readministration of adeno-associated viral vectors. Hum. Gene Ther. 9 (1998) 477–485.
11. M.Y. Mastakov, K. Baer, R. Xu, H. Fitzsimons, M.J. During. Combined injection of rAAV with mannitol enhances gene expression in the rat brain.Mol. Ther. 3 (2001) 225–232.
12. M.Y. Mastakov, K. Baer, R.M. Kotin, M.J. During. Recombinant adeno-associated virus serotypes 2- and 5-mediated gene transfer in the mammalian brain: quantitative analysis of heparin co-infusion. Mol. Ther. 5 (2002) 371–380.
13. Auricchio, G. Kobinger, V. Anand, M. Hildinger, E. OÕCon- nor, A.M. Maguire, J.M. Wilson, J. Bennett. Exchange of surface proteins impacts on viral vector cellular specificity and transduction characteristics: the retina as a model. Hum. Mol. Genet. 10 (2001) 3075–3081.
14. Burger, C, Gorbatyuk, OS, Velardo, MJ, Peden, CS, Williams, P, Zolotukhin, S *et al*. (2004). Recombinant AAV viral vectors pseudotyped with viral capsids from serotypes 1, 2, and 5 display differential efficiency and cell tropism after delivery to different regions of the central nervous system. *Mol Ther* 10: 302–317.

15. A.F. Skorupa, K.J. Fisher, J.M. Wilson, M.K. Parente, J.H.Wolfe (1999). Sustained production of beta-glucuronidase from localized sites after AAV vector gene transfer results in widespread distribution of enzyme and reversal of lysosomal storage lesions in a large volume of brain in mucopolysaccharidosis VII mice. Exp. Neurol. 160 17–27.
16. R.J. Mandel, S.K. Spratt, R.O. Snyder, S.E. Leff (1997). Midbrain injection of recombinant adeno-associated virus encoding rat glial cell line-derived neurotrophic factor protects nigral neurons in a progressive 6-hydroxydopamine-induced degeneration model of Parkinson's disease in rats. Proc. Natl. Acad. Sci. USA 94 14083–14088.
17. M. Azzouz, A. Hottinger, J.C. Paterna, A.D. Zurn, P. Aebischer, H. Bueler (2000). Increased motoneuron survival and improved neuromuscular function in transgenic ALS mice after intraspinal injection of an adeno-associated virus encoding Bcl-2.Hum. Mol. Genet. 9 803–811.
18. H. Okada, K. Miyamura, T. Itoh, M. Hagiwara, T. Wakabayashi, M. Mizuno, P. Colosi, G. Kurtzman, J. Yoshida, (1996). Gene Ther. 3 957–964.
19. Stoddard BL. 2011. Homing endonucleases: from microbial genetic in- vaders to reagents for targeted DNA modification. Structure 19:7–15.
20. Nesburn, AB. Vision Research – A National Plan, 1994–1998. US Department of Health and Human Services, Public Health Service, National Institutes of Health and the National Eye Institute; Bethesda, MD, USA: 1997. Report of the corneal disease panel; p. 138-146.
21. Roizman, B.; Knipe, DM.; Whitley, RJ. Herpes simplex viruses. Fields Virology. 5th Edition. Lippincott Williams & Wilkins; Baltimore, MD, USA: 2007. p. 2503-2602.

22. Ball MJ, Mathews R, Steiner I, et al. Latent HSV 1 virus in trigeminal ganglia: the optimal site for linking prevention of Alzheimer's disease to vaccination. Neurobiol. Aging. 2001; 22(5):705– 709.

23. Cohrs RJ, Randall J, Smith J, et al. Analysis of individual human trigeminal ganglia for latent herpes simplex virus type 1 and varicella-zoster virus nucleic acids using real-time PCR. J. Virol. 2000; 74(24):11464–11471.

24. Liedtke W, Opalka B, Zimmermann CW, Lignitz E. Age distribution of latent herpes simplex virus 1 and varicella-zoster virus genome in human nervous tissue. J. Neurol. Sci. 1993; 116(1):6–11.

25. Verjans GM, Hintzen RQ, van Dun JM, et al. Selective retention of herpes simplex virus-specific T cells in latently infected human trigeminal ganglia. Proc. Natl Acad. Sci. USA. 2007; 104(9): 3496–3501.

26. Cunningham AL, Diefenbach RJ, Miranda-Saksena M, et al. The cycle of human herpes simplex virus infection: virus transport and immune control. J. Infect. Dis. 2006; 194(Suppl. 1):S11–S18.

27. Pica F, Volpi A, Gaziano R, Garaci. Interferon-lambda in immunocompetent individuals with a history of recurrent herpes labialis. Antivir. Ther. 2010; 15(5):737–743.

28. Kramer MF, Chen SH, Knipe DM, Coen DM. Accumulation of viral transcripts and DNA during establishment of latency by herpes simplex virus. J. Virol. 1998; 72(2):1177–1185.

29. Javier RT, Stevens JG, Dissette VB, Wagner EK. A herpes simplex virus transcript abundant in latently infected neurons is dispensable for establishment of the latent state. Virology. 1988; 166(1):254–257.

30. Bloom DC. HSV LAT and neuronal survival. Int. Rev. Immunol. 2004; 23(1–2):187–198.

31. Bloom, DC. HSV-1 latency and the roles of the LATs. Alpha Herpesviruses: Molecular and Cellular Biology. First Edition. Caister Academic Press; Norwich, UK: 2006. p. 325-342.

32. Wu TT, Su YH, Block TM, Taylor JM. Evidence that two latency-associated transcripts of herpes simplex virus type 1 are nonlinear. J. Virol. 1996; 70(9):5962–5967.

33. Sawtell NM, Thompson RL. Herpes simplex virus type 1 latency-associated transcription unit promotes anatomical site-dependent establishment and reactivation from latency. J. Virol. 1992; 66(4):2157–2169.

34. Berthomme H, Lokensgard J, Yang L, Margolis T, Feldman LT. Evidence for a bidirectional element located downstream from the herpes simplex virus type 1 latency-associated promoter that increases its activity during latency. J. Virol. 2000; 74(8):3613–3622.

35. S. D. Cook, M. J. Paveloff, J. J. Doucet, A. J. Cottingham, F. Sedarati, and J. M. Hill, "Ocular herpes simplex virus reactivation in mice latently infected with latency-associated transcript mutants," Investigative Ophthalmology and Visual Science, vol. 32, no. 5, pp. 1558–1561, 1991.

36. Perng GC, Jones C. Towards an understanding of the herpes simplex virus type 1 latency-reactivation cycle. Interdiscip. Perspect. Infect. Dis. 2010:262415.

37. Hill JM, Gebhardt BM, Wen RJ, et al. Quantitation of herpes simplex virus type 1 DNA and latency-associated transcripts in rabbit trigeminal ganglia demonstrates a stable reservoir of viral nucleic acids during latency. J. Virol. 1996; 70(5):3137–3141.

38. C. Shimeld, T. J. Hill, W. A. Blyth, and D. L. Easty, "Reactivation of latent infection and induction of recurrent herpetic eye disease in mice," Journal of General Virology, vol. 71, no. 2, pp. 397–404, 1990.

39. Sawtell NM, Thompson RL (1992). Rapid in vivo reactivation of herpes simplex virus in latently infected murine ganglionic neurons after transient hyperthermia. J Virol 66: 2150– 2156.

40. Sawtell NM (1997). Comprehensive quantification of herpes simplex virus latency at the single-cell level. J Virol 71: 5423–5431.

41. Sawtell NM, Poon DK, Tansky CS, Thompson RL (1998). The latent herpes simplex virus type 1 genome copy number in individual neurons is virus strain specific and correlates with reactivation. J Virol 72: 5343–5350.

42. Kaplitt, MG, Leone, P, Samulski, RJ, Xiao, X, Pfaff, DW, O'Malley, KL *et al*. (1994). Long-term gene expression and phenotypic correction using adeno-associated virus vectors in the mammalian brain. *Nat Genet* 8: 148–154.

43. McCown, TJ, Xiao, X, Li, J, Breese, GR and Samulski, RJ (1996). Differential and persistent expression patterns of CNS gene transfer by an adeno-associated virus (AAV) vector. *Brain Res* 713: 99–107.

44. Peel, AL, Zolotukhin, S, Schrimsher, GW, Muzyczka, N and Reier, PJ (1997). Efficient transduction of green fluorescent protein in spinal cord neurons using adeno- associated virus vectors containing cell type-specific promoters. *Gene Ther* 4: 16–24.

45. Klein, RL, Meyer, EM, Peel, AL, Zolotukhin, S, Meyers, C, Muzyczka, N *et al*. (1998). Neuron-specific transduction in the rat septohippocampal or nigrostriatal pathway by recombinant adeno-associated virus vectors. *Exp Neurol* 150: 183–194.

46. Peel, AL and Klein, RL (2000). Adeno-associated virus vectors: activity and applications in the CNS. *J Neurosci Methods* 98: 95–104.

47. Ruitenberg, MJ, Eggers, R, Boer, GJ and Verhaagen, J (2002). Adeno-associated viral vectors as agents for gene delivery: application in disorders and trauma of the central nervous system. *Methods* 28: 182–194.

48. Kaplitt, MG, Feigin, A, Tang, C, Fitzsimons, HL, Mattis, P, Lawlor, PA *et al*. (2007). Safety and tolerability of gene therapy with an adeno-associated virus (AAV) borne GAD gene for Parkinson's disease: an open label, phase I trial. *Lancet* 369: 2097–2105.

49. Bainbridge, JW, Smith, AJ, Barker, SS, Robbie, S, Henderson, R, Balaggan, K *et al*. (2008). Effect of gene therapy on visual function in Leber's congenital amaurosis. *N Engl J Med* 358: 2231–2239.

50. Mandel, RJ and Burger, C (2004). Clinical trials in neurological disorders using AAV vectors: promises and challenges. *Curr Opin Mol Ther* 6: 482–490.

51. Arvanitakis, Z, Tuszynski, MH, Potkin, S, Bartus, R and Bennett, D (2009). A phase 1 clinical trial of CERE-110 (AAV-NGF) gene delivery in Alzheimer's disease. American Academy of Neurology Annual Meeting, Boston, MA, May 2007.

52. Glatzel, M, Flechsig, E, Navarro, B, Klein, MA, Paterna, JC, Buëler, H *et al*. (2000). Adenoviral and adeno-associated viral transfer of genes to the peripheral nervous system. *Proc Natl Acad Sci USA* 97: 442–447.

53. Xu, Y, Gu, Y, Wu, P, Li, GW and Huang, LY (2003). Efficiencies of transgene expression in nociceptive neurons through different routes of delivery of adeno-associated viral vectors. *Hum Gene Ther* 14: 897–906.

54. Xu, Y, Gu, Y, Xu, GY, Wu, P, Li, GW and Huang, LY (2003). Adeno-associated viral

transfer of opioid receptor gene to primary sensory neurons: a strategy to increase opioid antinociception. *Proc Natl Acad Sci USA* 100: 6204–6209.

55. Rutledge, EA, Halbert, CL and Russell, DW (1998). Infectious clones and vectors derived from adeno-associated virus (AAV) serotypes other than AAV type 2. *J Virol* 72: 309–319.

56. Xiao, W, Chirmule, N, Berta, SC, McCullough, B, Gao, G and Wilson, JM (1999). Gene therapy vectors based on adeno-associated virus type 1. *J Virol* 73: 3994–4003.

57. Chao, H, Liu, Y, Rabinowitz, J, Li, C, Samulski, RJ and Walsh, CE (2000). Several log increase in therapeutic transgene delivery by distinct adeno-associated viral serotype vectors. *Mol Ther* 2: 619–623.

58. Rabinowitz, JE, Rolling, F, Li, C, Conrath, H, Xiao, W, Xiao, X *et al*. (2002). Cross-packaging of a single adeno-associated virus (AAV) type 2 vector genome into multiple AAV serotypes enables transduction with broad specificity. *J Virol* 76: 791–801.

59. Gao, GP, Alvira, MR, Wang, L, Calcedo, R, Johnston, J and Wilson, JM (2002). Novel adeno-associated viruses from rhesus monkeys as vectors for human gene therapy. *Proc Natl Acad Sci USA* 99: 11854–11859.

60. Wang, C, Wang, CM, Clark, KR and Sferra, TJ (2003). Recombinant AAV serotype 1 transduction efficiency and tropism in the murine brain. *Gene Ther* 10: 1528–1534.

61. Paterna, JC, Feldon, J and Büeler, H (2004). Transduction profiles of recombinant adeno-associated virus vectors derived from serotypes 2 and 5 in the nigrostriatal system of rats. *J Virol* 78: 6808–6817.

62. Burger, C, Gorbatyuk, OS, Velardo, MJ, Peden, CS, Williams, P, Zolotukhin, S *et al*. (2004). Recombinant AAV viral vectors pseudotyped with viral capsids from serotypes 1,

2, and 5 display differential efficiency and cell tropism after delivery to different regions of the central nervous system. *Mol Ther* 10: 302–317.

63. Klein, RL, Dayton, RD, Leidenheimer, NJ, Jansen, K, Golde, TE and Zweig, RM (2006). Efficient neuronal gene transfer with AAV8 leads to neurotoxic levels of tau or green fluorescent proteins. *Mol Ther* 13: 517–527.

64. Storek, B, Reinhardt, M, Wang, C, Janssen, WG, Harder, NM, Banck, MS *et al*. (2008). Sensory neuron targeting by self-complementary AAV8 via lumbar puncture for chronic pain. *Proc Natl Acad Sci USA* 105: 1055–1060.

65. Storek, B, Harder, NM, Banck, MS, Wang, C, McCarty, DM, Janssen, WG *et al*. (2006). Intrathecal long-term gene expression by self-complementary adeno-associated virus type 1 suitable for chronic pain studies in rats. *Mol Pain* 2: 4.

66. Towne, C, Pertin, M, Beggah, AT, Aebischer, P and Decosterd, I (2009). Recombinant adeno-associated virus serotype 6 (rAAV2/6)-mediated gene transfer to nociceptive neurons through different routes of delivery. *Mol Pain* 5: 52.

67. .Taymans, JM, Vandenberghe, LH, Haute, CV, Thiry, I, Deroose, CM, Mortelmans, L *et al*. (2007). Comparative analysis of adeno-associated viral vector serotypes 1, 2, 5, 7, and 8 in mouse brain. *Hum Gene Ther* 18: 195–206.

68. Chen, S., Kapturczak, M., Loiler, S. A., Zolotukhin, S., Glushakova, O. Y., Madsen, K. M., Samulski, R. J., Hauswirth, W. W., Campbell-Thompson, M., Berns, K. I., Flotte, T. R., Atkinson, M. A., Tisher, C. C., and Agarwal, A. (2005) Efficient transduction of vascular endothelial cells with recombinant adeno-associated virus serotype 1 and 5 vectors, *Hum Gene Ther 16*, 235–247.51.

69. Wu, Z., Miller, E., Agbandje-McKenna, M., and Samulski, R. J. (2006) Alpha2,3 and

alpha2,6 N-linked sialic acids facilitate efficient binding and transduction by adeno-associated virus types 1 and 6, *J Virol 80*, 9093–9103.52. Kaludov, N., Brown, K. E., Walters, R. W.,

70. Zabner, J., and Chiorini, J. A. (2001). Adeno-associated virus serotype 4 (AAV4) and AAV5 both require sialic acid binding for hemagglutination and efficient transduction but differ in sialic acid linkage specificity, *J Virol 75*, 6884–6893.

71. Walters, R. W., Yi, S. M., Keshavjee, S., Brown, K. E., Welsh, M. J., Chiorini, J. A., and Zabner, J. (2001). Binding of adeno-associated virus type 5 to 2,3-linked sialic acid is required for gene transfer, *J Biol Chem 276*, 20610–20616.

72. Di Pasquale, G., Davidson, B. L., Stein, C. S., Martins, I., Scudiero, D., Monks, A., and Chiorini, J. A. (2003) Identification of PDGFR as a receptor for AAV-5 transduction, *Nat Med 9*, 1306–1312.

73. Wu, Z., Asokan, A., Grieger, J. C., Govindasamy, L., Agbandje-McKenna, M., and Samulski, R. J. (2006). Single amino acid changes can influence titer, heparin binding, and tissue tropism in different adeno- associated virus serotypes, *J Virol 80*, 11393–11397.

74. Aschauer DF, Kreuz S, Rumpel S (2013). Analysis of Transduction Efficiency, Tropism and Axonal Transport of AAV Serotypes 1, 2, 5, 6, 8 and 9 in the Mouse Brain. PLoS ONE 8(9): e76310. doi:10.1371/journal.pone.0076310

75. Klug, A. (2010). The discovery of zinc fingers and their applications in gene regulation and genome manipulation. Annu. Rev. Biochem. 79, 213–231.

76. Gaj, T., Gersbach, C.A., Barbas 3rd, C.F. (2013). ZFN, TALEN, and CRISPR/Cas-based methods for genome engineering. Trends Biotechnol. 31, 397–405.

77. Christian, M., Cermak, T., Doyle, E.L., Schmidt, C., Zhang, F., Hummel, A., Bogdanove, A.J., Voytas, D.F. (2010). Targeting DNA double-strand breaks with TAL effector nucleases. Genetics 186, 757–761.

78. Miller, J.C., Tan, S., Qiao, G., Barlow, K.A., Wang, J., Xia, D.F., Meng, X., Paschon, D.E., Leung, E., Hinkley, S.J., Dulay, G.P., Hua, K.L., Ankoudinova, I., Cost, G.J., Urnov, F.D., Zhang, H.S., Holmes, M.C., Zhang, L., Gregory, P.D., Rebar, E.J. (2011). A TALE nuclease architecture for efficient genome editing. Nat. Biotechnol. 29, 143–148.

79. Barrangou, R., Marraffini, L.A. (2014). CRISPR-Cas systems: prokaryotes upgrade to adaptive immunity. Mol. Cell. 54, 234–244.

80. Cong, L., Ran, F.A., Cox, D., Lin, S., Barretto, R., Habib, N., Hsu, P.D., Wu, X., Jiang, W., Marraffini, L.A., Zhang, F. (2013). Multiplex genome engineering using CRISPR/Cas systems. Science 339, 819–823.

81. Hsu, P.D., Scott, D.A., Weinstein, J.A., Ran, F.A., Konermann, S., Agarwala, V., Li, Y., Fine, E.J., Wu, X., Shalem, O., Cradick, T.J., Marraffini, L.A., Bao, G., Zhang, F. (2013). DNA targeting specificity of RNA-guided Cas9 nucleases. Nat. Biotechnol. 31, 827–832.

82. Kutluay SB & Triezenberg SJ (2009). Role of chromatin during herpesvirus infections. Biochim Biophys Acta 1790: 456–466.

83. Bloom DC, Giordani NV & Kwiatkowski DL (2010). Epigenetic regulation of latent HSV-1 gene expression. Biochim Biophys Acta 1799: 246–256.

84. Herrera FJ & Triezenberg SJ (2004). VP16-dependent association of chromatin-modifying coactivators and underrepresentation of histones at immediate-early gene promoters during herpes simplex virus infection. J Virol 78: 9689–9696.

85. Arthur JL, Scarpini CG, Connor V, Lachmann RH, Tolkovsky AM, Efstathiou S (2001). Herpes simplex virus type 1 promoter activity during latency establish- ment, maintenance, and reactivation in primary dorsal root neurons in vitro. J Virol 75: 3885–3895.

86. Kubat NJ, Tran RK, McAnany P & Bloom DC (2004) Specific histone tail modification and not DNA methylation is a determinant of herpes simplex virus type 1 latent gene expression. J Virol 78: 1139–1149.

87. Knipe DM & Cliffe A (2008). Chromatin control of herpes simplex virus lytic and latent infection. Nat Rev Microbiol 6: 211–221.

88. Zhu, J., D. M. Koelle, J. Cao, J. Vazquez, M. L. Huang, F. Hladik, A. Wald, and L. Corey (2007). Virus-specific CD8+ T cells accumulate near sensory nerve endings in genital skin during subclinical HSV-2 reactivation. J. Exp. Med. 204:595–603.

89. Khanna, K. M., R. H. Bonneau, P. R. Kinchington, and R. L. Hendricks (2003). Herpes simplex virus-specific memory CD8+ T cells are selectively activated and retained in latently infected sensory ganglia. Immunity 18: 593–603.

90. Aubert M., Boyle N.M, Stone D., Stensland,L., Huang M.L, Magaret A.S., Galetto R., Rawlings D.J., Scharenberg A.M., Jerome K.R. (2014). In vitro inactivation of latent HSV by targeted mutagenesis using an HSV-specific homing endonuclease. Mol Ther Nucleic Acids. Feb 4; 3.

91. Weber N.M., Stone D., Sedlak R.H., De Silva Feelixge H.S., Roychoudhury P., Schiffer J.T., Aubert M., Jerome K.R. (2014). AAV-mediated delivery of zinc finger nucleases targeting hepatitis B virus inhibits active replication. PLoS One. May 14; 9(5).